SIAM J. NUMER. ANAL.
Vol. 55, No. 4, pp. 1892–1914

ABOUT SOME BOUNDARY INTEGRAL OPERATORS ON THE UNIT DISK RELATED TO THE LAPLACE EQUATION*

PEDRO RAMACIOTTI† AND JEAN-CLAUDE NÉDÉLEC‡

Abstract. We introduce four integral operators related to the Laplace equation in three dimensions on the circular unit disk. Two of them are related to the weakly singular operator and the other two are related to the hypersingular operator. We provide series expressions for their kernels using proposed bases for the Sobolev trace spaces involved in the symmetric Dirichlet and antisymmetric Neumann Laplace screen problems on the disk. We then provide explicit and closed variational forms suitable for boundary element computations. We develop numerical computation schemes for the associated Galerkin matrices and test their use as preconditioners for the matrices arising from the integral equations associated with the solution of the mentioned screen problems.

Key words. open surface problem, boundary integral operators, boundary element methods, preconditioners for iterative methods

AMS subject classifications. 45P05, 65N38, 65N12, 31A10, 46E35, 65F08

DOI. 10.1137/15M1033721

1. Introduction.

We consider the boundary integral operators related to the Dirichlet and Neumann boundary value problems for the exterior Laplace problem (1). The results for the Helmholtz problems follow as a compact perturbation of this case. Applications of such problems arise in many physical contexts. The Dirichlet or Neumann Laplace problem for the exterior of an obstacle $\Omega \subset \mathbb{R}^3$ embedded in a three-dimensional space can be stated as

$$\text{(1)} \qquad \begin{cases} -\Delta u = 0 \text{ in } \mathbb{R}^3 \setminus \overline{\Omega}, \\ u = g \text{ or } \dfrac{\partial u}{\partial n} = \varphi \text{ on } \Gamma = \partial\Omega, \end{cases}$$

for suitable spaces defined over $\mathbb{R}^3 \setminus \overline{\Omega}$ for u and over Γ for g or φ. When solving these problems in unbounded homogeneous exterior domains, boundary element methods are a suitable option because they respect the physical behavior at infinity and because they only require the boundaries to be meshed, in contrast with the so-called domain methods. The boundary element methods first convert the partial differential equations to first kind boundary integral equations, which can then be solved numerically [12, 14, 7]. The resulting boundary integral equations are linked to the weakly singular and hypersingular boundary integral operators

$$\text{(2)} \quad (\mathcal{S}\lambda)(\mathbf{y}) = \int_\Gamma G(\mathbf{x},\mathbf{y})\lambda(\mathbf{x})d\Gamma(\mathbf{x}) \quad \text{and} \quad (\mathcal{N}\mu)(\mathbf{y}) = \int_\Gamma \frac{\partial^2 G}{\partial n_{\mathbf{x}} \partial n_{\mathbf{y}}}(\mathbf{x},\mathbf{y})\mu(\mathbf{x})d\Gamma(\mathbf{x}),$$

*Received by the editors August 3, 2015; accepted for publication (in revised form) March 9, 2017; published electronically August 3, 2017.
http://www.siam.org/journals/sinum/55-4/M103372.html
Funding: The work of the authors was supported by Labex LMH through grant ANR-11-LABX-0056-LMH in "Programme des Investissements d'Avenir" and MECE Educación Superior PUC0710.

†CMAP, École Polytechnique, CNRS, Université Paris–Saclay, 91128 Palaiseau, France, and Facultad de Ingeniería, Pontificia Universidad Católica de Chile, 4860 Santiago, Chile (pedro.ramaciotti@polytechnique.edu).
‡CMAP, École Polytechnique, CNRS, Université Paris–Saclay, 91128, Palaiseau, France (jean-claude.nedelec@polytechnique.edu).

where $G(\mathbf{x},\mathbf{y}) = (4\pi\|\mathbf{x}-\mathbf{y}\|)^{-1}$ is the associated Green's function for the Laplace equation, and λ and μ functions defined over Γ.

The Galerkin matrices arising from the variational formulations for the related boundary integral equations are dense, and thus the algorithmic and memory complexity is elevated for the resolution of the associated linear systems. This is even more relevant in three dimensions. The algorithmic and memory complexity can be treated with compression and acceleration methods such as the fast multipole method, the panel clustering method, or the hierarchical matrix method with adaptive cross approximation methods. But these techniques rely on iterative solvers, for which the control of the number of iterations, and thus the control of the condition number of the associated matrix, becomes crucial in providing low complexity, high accuracy methods. In the case of the first kind boundary integral equations it can be proved that the spectral condition number will grow as $\mathcal{O}(h^{-1})$, where h is the smallest cell of mesh [16, section 3.5.3], making preconditioning indispensable. Also, the accuracy of the results depends on the condition number when there are numerical errors in the computations of the elements of the matrix and the right-hand-side vectors [2, section 2.6.2]. This provides additional motivation for the improvement of the condition number.

When the obstacle Ω has a Lipschitz-regular boundary Γ, Dirichlet and Neumann trace spaces are dual to each other. The weakly singular and the hypersingular boundary integral operators (2) induce linear, continuous, and coercive bilinear variational forms that give rise to Galerkin matrices that act as mutual optimal preconditioners [4]. In this case, low condition numbers are ensured by the Calderón identities. When the domain is not Lipschitz-regular, e.g., in the case of a screen problem, when the interior domain is void and the surface Γ is not closed ($\partial\Gamma \neq \varnothing$), the mapping properties of the weakly singular and the hypersingular boundary integral operators degenerate: the trace spaces associated with them are no longer dual to each other, the Calderón identities no longer hold, and the Galerkin matrices no longer provide optimal mutual preconditioning. The so-called screen problems have, however, numerous applications, such as in crack problems in mechanics [15, 13] and antenna and printed circuit board models [17].

Different approaches have been tried to tackle this problem. Despite the fact that the Calderón identities no longer hold for screen boundaries, the weakly singular and the hypersingular boundary integral operators do precondition each other to some degree, as proposed in [11], although not in an asymptotically optimal manner, with the spectral condition number growing as $\mathcal{O}(|\log h|)$. Another approach, called the generalized Calderón formula for open boundaries, provides good preconditioning tools [10], but no asymptotical estimations are available.

Recently, explicit variational inverses have been found by Jerez-Hanckes and Nédélec for the boundary integral operators (2), along with precise space mapping properties and Calderón-type identities for the segment screen ($\Gamma = (-1,1)\times\{0\}$) in $\mathbb{R}^2$ [8]. These inverse operators induce linear, continuous, and coercive bilinear variational forms in the dual spaces for each operator and thus provide a means to build preconditioning Galerkin matrices [5]. These results have also been proved to be extensible to the boundary integral operators linked to the Helmholtz equation and to curves other than the segment via a sufficiently regular curve transformation.

In this article we propose new boundary integral operators for the case disk screen in $\mathbb{R}^3$ extending key properties of the inverse ones proposed for two dimensions in [8], now into three dimensions. First we describe the geometrical and functional framework of the problem. Then we consider appropriate basis functions to develop

series expressions of the distributions of the relevant trace spaces involved in the Laplace problems. We use these series expressions to propose new boundary integral operators on the disk in $\mathbb{R}^3$ that aim to preserve some key features of the ones previously proposed for the segment in $\mathbb{R}^2$. We provide Calderón-type identities for these operators and we develop explicit and closed variational forms for them, suitable for boundary element computations. Finally, we use these boundary element computations to build Galerkin matrices and test the preconditioning action of these boundary integral operators when applied to the matrices involved in the resolution of the Dirichlet and Neumann Laplace screen problem.

2. Geometrical and functional framework.

2.1. Geometrical setting. Let $\mathbf{x} = (x_1, x_2, x_3) \in \mathbb{R}^3$ be a point in three-dimensional space. We take interest in the unit disk in $\mathbb{R}^3$: $\mathbb{D} = \{\mathbf{x} \in \mathbb{R}^3 : x_3 = 0, x_1^2 + x_2^2 < 1\}$. The domain for the Laplace Dirichlet of Neumann obstacle problem for the unit disk screen obstacle is denoted by $\Omega_{\mathbb{D}} = \mathbb{R}^3 \setminus \overline{\mathbb{D}}$.

We also consider the unit sphere $\mathbb{S}$ in $\mathbb{R}^3$. The plane $\pi = \{\mathbf{x} : x_3 = 0\}$ divides the unit sphere into the upper half-sphere $\mathbb{S}^+$ and the lower half-sphere $\mathbb{S}^-$. For a point on $\mathbb{S}$, we consider the spherical coordinate system (θ, ϕ), where θ and ϕ are the classical Euler angles ($\theta \in [0, \pi]$ and $\phi \in [0, 2\pi]$):

$$\begin{cases} x_1(\theta,\phi) = \sin\theta\cos\phi, \\ x_2(\theta,\phi) = \sin\theta\sin\phi, \\ x_3(\theta,\phi) = \cos\theta, \end{cases} \qquad \begin{cases} \theta(\mathbf{x}) = \theta_{\mathbf{x}} = \arccos(x_3), \\ \phi(\mathbf{x}) = \phi_{\mathbf{x}} = \arctan(x_2/x_1), \end{cases}$$

For a point on the disk in Cartesian coordinates $(x_1, x_2) \in \mathbb{R}^2$ we also consider cylindrical coordinates (ρ, ϕ), where ρ is the radius.

$$\begin{cases} x_1(\rho,\phi) = \rho\cos\phi, \\ x_2(\rho,\phi) = \rho\sin\phi, \end{cases} \qquad \begin{cases} \rho(\mathbf{x}) = \rho_{\mathbf{x}} = \sqrt{x_1^2 + x_2^2} = \sin\theta, \\ \phi(\mathbf{x}) = \phi_{\mathbf{x}} = \arctan(x_2/x_1). \end{cases}$$

To a point $\mathbf{x} \in \mathbb{D}$ we associate $\mathbf{x}^\pm \in \mathbb{S}^\pm$, the vertical projection onto the upper and lower half-spheres. Likewise, points $\mathbf{x}^\pm \in \mathbb{S}^\pm$ have a vertical projection $\mathbf{x} \in \mathbb{D}$ onto the disk.

We define a function $w(\rho) = \sqrt{1-\rho^2} = \cos\theta$, also $w(\mathbf{x}) = \sqrt{1-\rho_{\mathbf{x}}^2}$, relating the radius ρ of a point $\mathbf{x} \in \mathbb{D}$ with the distance to its vertical projections on the unit sphere $\mathbb{S}$, such that, for $\mathbf{x} = (\rho, \phi) \in \mathbb{D}$, $\mathbf{x}^\pm(\rho, \phi) = (\rho\cos\phi, \rho\sin\phi, \pm w(\rho))$.

2.2. Sobolev trace spaces for the disk in $\mathbb{R}^3$. Using the usual notation for Sobolev spaces, for any $s > 0$, $\widetilde{H}^s(\mathbb{D})$ is the space of distributions whose extension by zero to π belongs to $H^s(\pi)$. It is noteworthy that $\widetilde{H}^{1/2}(\mathbb{D}) \subseteq H_0^{1/2}(\mathbb{D})$. We identify

$$\widetilde{H}^{-1/2}(\mathbb{D}) \equiv \left(H^{1/2}(\mathbb{D})\right)' \qquad \text{and} \qquad H^{-1/2}(\mathbb{D}) \equiv \left(\widetilde{H}^{1/2}(\mathbb{D})\right)',$$

where prime designates a dual space. Duality pairings on the disk are written with angular brackets $\langle\cdot,\cdot\rangle_{\mathbb{D}}$, and inner products with parentheses $(\cdot,\cdot)$, both sesquilinear. Relations of inclusion between the identified spaces are given by [18]

$$\tilde{H}^{1/2}(\mathbb{D}) \subset L^2(\mathbb{D}) \subset H^{-1/2}(\mathbb{D}), \quad H^{1/2}(\mathbb{D}) \subset L^2(\mathbb{D}) \subset \tilde{H}^{-1/2}(\mathbb{D}).$$

2.3. Preconditioning. The symmetric Neumann and antisymmetric Dirichlet Laplace screen problems do not require recasting as boundary integral equations; one just introduces the Dirichlet and Neumann data respectively into the single layer and

double layer integral potential operator [14, equations 3.1.33 and 3.1.34] to compute the solution u to the problem (1) in the whole problem domain. When considering the symmetric Dirichlet and antisymmetric Neumann screen problems, we need to make use of boundary integral operators (2) to recast the problem as boundary integral equations. Indeed, given the Dirichlet data $g \in H^{1/2}(\mathbb{D})$, a function u is the solution in $H^1_{loc}(\Omega_{\mathbb{D}})$ to the Dirichlet problem if and only if the jump of the Neumann trace across $\mathbb{D}$, i.e., if $\lambda = [\partial u/\partial n]$ solves $\mathcal{S}\lambda = g$ [19, Theorem 2.5]. Similarly, given the Neumann data $\varphi \in H^{-1/2}(\mathbb{D})$, a function u is the solution in $H^1_{loc}(\Omega_{\mathbb{D}})$ to the Neumann problem if and only if the jump of the Dirichlet trace across $\mathbb{D}$, i.e., if $\mu = [u]$ solves $-\mathcal{N}\mu = \varphi$ [19, Theorem 2.6]. We also know that if $u \in H^1_{loc}(\Omega_{\mathbb{D}})$ is the solution to (1), its traces are such that $\lambda \in \widetilde{H}^{-1/2}(\mathbb{D})$ and $\mu \in \widetilde{H}^{1/2}(\mathbb{D})$ [19, Theorem 2.2]. This impedes mutual optimal operator preconditioning, as becomes clear in light of the following theorem.

THEOREM 2.1 (operator preconditioning [4, Theorem 2.1]). *Let V and W be reflexive Banach spaces. Let $a \in L(V \times V, \mathbb{C})$, $b \in L(W \times W, \mathbb{C})$, and $d \in L(V \times W, \mathbb{C})$ be continous sesquilinear forms. Finally, let $V_h = span(\{\chi_i\}_{i=1}^N) \subset V$ and $W_h = span(\{\kappa_i\}_{i=1}^N) \subset W$ be finite-dimensional subspaces of the same dimension on which the following* inf-sup *conditions are fulfilled:*

$$\forall u_h \in V_h \sup_{v_h \in V_h} \frac{|a(u_h, v_h)|}{\|v_h\|_V} \geq c_a \|u_h\|_V, \quad \forall q_h \in W_h \sup_{w_h \in W_h} \frac{|b(q_h, w_h)|}{\|w_h\|_W} \geq c_b \|q_h\|_W,$$
$$\forall v_h \in V_h \sup_{w_h \in W_h} \frac{|d(v_h, w_h)|}{\|w_h\|_W} \geq c_d \|v_h\|_V. \tag{3}$$

Let us define the Galerkin matrices $\boldsymbol{A}[i,j] = a(\chi_i, \chi_j)$, $\boldsymbol{B}[i,j] = b(\kappa_i, \kappa_j)$, and $\boldsymbol{D}[i,j] = d(\chi_i, \kappa_j)$, and let us define the preconditioning matrix $\boldsymbol{M} = \boldsymbol{D}^{-1}\boldsymbol{B}\boldsymbol{D}^{-H}$. The spectral condition number of the preconditioned matrix $\boldsymbol{M}\boldsymbol{A}$ has the following bound: $cond_2(\boldsymbol{M}\boldsymbol{A}) \leq \frac{\|a\|\|b\|\|d\|^2}{c_a c_b c_d^2}$.

When posed over Lipschitz-regular surfaces Γ, boundary integral operators $\mathcal{S}$ and $\mathcal{N}$ induce continuous sesquilinear forms in $H^{-1/2}(\Gamma)$ and $H^{1/2}(\Gamma)$, which are mutual dual spaces. Considering zeroth and first order Lagrange finite elements supported by triangular primary and polygonal dual meshes as in [18, section 2.2] (which we revisit in section 4.1) satisfies condition (3) of the theorem while providing finite subspaces with the same dimensions. All these conditions satisfy the hypotheses of the previous theorem, thus yielding optimal preconditioning.

As seen before, this approach no longer applies when Γ is a screen, in particular $\mathbb{D}$. In the case of the screen obstacle, operators $\mathcal{S}$ and $\mathcal{N}$ map trace spaces into their duals, inducing coercive bilinear forms, but the spaces do not coincide: we have four spaces instead of two. A possible solution is finding inverses to these operators to use in operator preconditioning. This is, in general, a difficult goal. It has been achieved for the segment screen in $\mathbb{R}^2$ in [8] and more recently for the disk in $\mathbb{R}^3$ but only for $\mathcal{N}$. This exact inverse (derived in $\mathbb{R}^3$ using additional tools, most notably [9]) induces a coercive, continuous bilinear form in $H^{-1/2}(\mathbb{D})$, thus providing an optimal preconditioner, as has been tested in numerical experiments [6]. By contrast, the new operators presented in this article are not the inverses of $\mathcal{S}$ and $\mathcal{N}$. They have been conceived to mimic the key properties that allowed for improvement of the condition number in the case of the segment in $\mathbb{R}^2$. These properties are related to singular behavior near the edge of the screen, described by the function w. For the segment screen in $\mathbb{R}^2$, the weakly singular kernel of the inverse integral operator $\mathcal{N}^{-1}$, denoted

K_{as}^{ws}, and the hypersingular kernel of the inverse operator $\mathcal{S}^{-1}$, denoted K_s^{hs}, had the following series expressions:

$$(4)\quad K_{as}^{ws}(x,y)=\sum_{n=1}^{\infty}\frac{w(x)w(y)}{n}U_{n-1}(x)U_{n-1}(y)\quad\text{and}\quad K_s^{hs}(x,y)=\sum_{n=1}^{\infty}2n\frac{T_n(x)T_n(y)}{w(x)w(y)},$$

where now $w(x)=\sqrt{1-x^2}$, and T_n and U_n are the first and second kind Tchebyshev polynomials. We take the behavior of these kernels as hints for the proposal of new boundary integral operators on the disk that play a similar role in an operator preconditioning technique.

3. Some boundary integral operators on the disk. In order to specify the proposed boundary integral operators we make use of special basis functions defined on the disk. The definition of these functions are motivated by the following remark.

Remark 3.1 (jump of the traces near the edge of the disk). If u is the solution of the Laplace screen problem for the disk, the jump of the Neumann trace behaves as $\lambda\sim 1/\sqrt{1-\rho^2}$ near the edge, i.e., $\rho\sim 1$, and the jump of the Dirichlet trace behaves as $\mu\sim\sqrt{1-\rho^2}$ near the edge [19, Theorem 2.9].

3.1. Disk basis functions.

Definition 3.2 (vertical projection of the spherical harmonics). *We define the* $2l+1$ *disk basis functions of order* $l\geq 0$ *on* $\mathbb{D}$ *as*

$$y_l^m(\mathbf{x})=y_l^m(\rho,\phi)=\gamma_l^m e^{\mathrm{i}m\phi}\mathbb{P}_l^m\left(w(\rho)\right)=\gamma_l^m e^{\mathrm{i}m\phi}\mathbb{P}_l^m\left(\cos\theta\right)=Y_l^m(\theta,\phi)=Y_l^m(\mathbf{x}^+)$$

for $-l\leq m\leq l$, *where* $\gamma_l^m=(-1)^m\sqrt{\frac{l+1/2}{2\pi}}\sqrt{\frac{(l-m)!}{(l+m)!}}$ *and* Y_l^m *is the spherical harmonic of order* l *and degree* m [14, section 2.4.3].

The disk basis functions have an orthogonality property on $\mathbb{D}$, inherited from the orthogonality of the spherical harmonics on $\mathbb{S}$.

Proposition 3.3 (orthogonality identity on $\mathbb{D}$). *If* l_1+m_1 *and* l_2+m_2 *have the same parity, the following orthogonality identity holds:*

$$\int_{\mathbb{D}}\frac{y_{l_1}^{m_1}(\mathbf{x})\overline{y_{l_2}^{m_2}(\mathbf{x})}}{w(\mathbf{x})}d\mathbb{D}(\mathbf{x})=\frac{1}{2}\delta_{m_2}^{m_1}\delta_{l_2}^{l_1}.$$

Proof. The change of variable $\rho=\sin\theta$, along with the identity $y_l^m(\rho,\phi)=Y_l^m(\theta(\mathbf{x}^+),\phi(\mathbf{x}^+))$, implies that

$$\begin{aligned}\int_{\mathbb{D}}\frac{y_{l_1}^{m_1}(\mathbf{x})\overline{y_{l_2}^{m_2}(\mathbf{x})}}{w(\mathbf{x})}d\mathbb{D}(\mathbf{x})&=\int_{\mathbb{S}^+}Y_{l_1}^{m_1}(\mathbf{x})\overline{Y_{l_2}^{m_2}(\mathbf{x})}d\mathbb{S}^+(\mathbf{x})\\&=\gamma_{l_1}^{m_1}\gamma_{l_2}^{m_2}2\pi\delta_{m_2}^{m_1}\int_0^1\mathbb{P}_{l_1}^{m_1}(t)\mathbb{P}_{l_2}^{m_2}(t)dt.\end{aligned}$$

Since l_1+m_1 and l_2+m_2 have the same parity, so do they have the two associated Legendre functions. Thus the last integral is equal to $1/2$ of the integral over $[-1,1]$ of the multiplied associated Legendre functions, yielding the desired results. ∎

Let us define some sets of basis functions that will be used in series representation of functions and kernels defined for the spaces defined in section 2.2.

DEFINITION 3.4 (symmetric and antisymmetric sets). *We define the following sets using the disk basis functions and the weight function w:*

$$\mathcal{Y}_s = \{y_l^m : -l \le m \le l, \text{ and } l+m \text{ is even}\}, \quad \mathcal{Y}_s^{1/w} = \left\{ \frac{y_l^m}{w} : y_l^m \in \mathcal{Y}_s \right\},$$
$$\mathcal{Y}_{as} = \{y_l^m : -l \le m \le l, \text{ and } l+m \text{ is odd}\}, \quad \mathcal{Y}_{as}^{1/w} = \left\{ \frac{y_l^m}{w} : y_l^m \in \mathcal{Y}_{as} \right\}.$$

Remark 3.5 (behavior of the disk basis functions in the radial direction). The functions from spaces $\mathcal{Y}_s$ and $\mathcal{Y}_{as}^{1/w}$ are polynomial in variable ρ in the radial direction. The functions from the space $\mathcal{Y}_{fas}$ are of the form $p(\rho)\sqrt{1-\rho^2}$ in the radial direction, where p is a polynomial. The functions from the space $\mathcal{Y}_s^{1/w}$ are of the form $p(\rho)/\sqrt{1-\rho^2}$ in the radial direction, where p is a polynomial.

DEFINITION 3.6 (sesquilinear forms associated with w and $1/w$). *Let us notate by $(\cdot,\cdot)_w$ and $(\cdot,\cdot)_{1/w}$ the following sesquilinear forms associated with the weight function w:*

$$(u,v)_w = \int_{\mathbb{D}} u(\mathbf{x})\overline{v(\mathbf{x})}w(\mathbf{x})d\mathbb{D}(\mathbf{x}) \quad \text{and} \quad (u,v)_{1/w} = \int_{\mathbb{D}} u(\mathbf{x})\overline{v(\mathbf{x})}w^{-1}(\mathbf{x})d\mathbb{D}(\mathbf{x}).$$

DEFINITION 3.7 (the $L^2_w(\mathbb{D})$ and the $L^2_{1/w}(\mathbb{D})$ spaces). *Let us define the space $L^2_w(\mathbb{D})$, associated with the inner product $(\cdot,\cdot)_w$ and to the norm $\|u\|_w = \sqrt{(u,u)_w}$, as*

$$L^2_w(\mathbb{D}) = \{u \text{ measurable } : \|u\|_w < \infty\}$$

and the space $L^2_{1/w}(\mathbb{D})$, associated with the inner product $(\cdot,\cdot)_{1/w}$ and to the norm $\|u\|_{1/w} = \sqrt{(u,u)_{1/w}}$, as

$$L^2_{1/w}(\mathbb{D}) = \left\{u \text{ measurable } : \|u\|_{1/w} < \infty\right\}.$$

PROPOSITION 3.8 (bases for $L^2_w(\mathbb{D})$ and $L^2_{1/w}(\mathbb{D})$). *The sets $\mathcal{Y}_s^{1/w}$ and $\mathcal{Y}_{as}^{1/w}$ form, each one, an orthogonal and complete basis for $L^2_w\mathbb{D}$. Likewise, the sets $\mathcal{Y}_s$ and $\mathcal{Y}_{as}$ form, each one, an orthogonal and complete basis for $L^2_{1/w}\mathbb{D}$.*

Proof. Orthogonality follows from Proposition 3.3. The sets $\mathcal{Y}_s^{1/w}$ and $\mathcal{Y}_{as}^{1/w}$ are subsets of $L^2_w(\mathbb{D})$, since they have a finite norm. If $\mathcal{Y}_s^{1/w}$ was not dense in $L^2_w(\mathbb{D})$, there would be a member $f \in L^2_w(\mathbb{D})$ not a.e. equal to zero and orthogonal to all members of $\mathcal{Y}_s^{1/w}$, i.e.,

$$\left(f\,,\,\frac{y_l^m}{w}\right)_w = \int_{\mathbb{D}} f(\mathbf{x})\overline{y_l^m(\mathbf{x})}d\mathbb{D}(\mathbf{x}) = 0 \text{ for } l \ge 0,\ -l \le m \le l,\ l+m \text{ even}.$$

But for $l+m$ even, the set of functions y_l^m is dense in $C^\infty(\mathbb{D})$. Thus f would be zero a.e., contradicting the premise. The same argument can be used for $l+m$ odd, except that y_l^m functions in the radial direction are $w(\rho)p(\rho)$, where now p is polynomial.

Similarly, $\mathcal{Y}_s$ and $\mathcal{Y}_{as}$ are subsets of $L^2_{1/w}(\mathbb{D})$. If $\mathcal{Y}_s$ was not dense in $L^2_{1/w}(\mathbb{D})$, there would be a member $f \in L^2_{1/w}(\mathbb{D})$ not a.e. equal to zero such that $(f\,,\,y_l^m)_{1/w} = 0$ for every $y_l^m \in \mathcal{Y}_s$. But following the previous reasoning, that would mean that f/w is zero a.e., thus also f itself. Extending the same reasoning to $\mathcal{Y}_{as}$ finishes the proof. ∎

Remark 3.9 (jump of the traces near the edge of the disk). Remarks 3.1 and 3.5 motivate the expansion of functions in $\widetilde{H}^{1/2}(\mathbb{D})$ on the space $L^2_{1/w}$ on the basis $\mathcal{Y}_{as}$, functions in the space $H^{1/2}(\mathbb{D})$ on the space $L^2_{1/w}$ on the basis $\mathcal{Y}_s$, functions in the space $H^{-1/2}(\mathbb{D})$ on the space L^2_w on the basis $\mathcal{Y}^{1/w}_{as}$, and functions in the space $\widetilde{H}^{-1/2}(\mathbb{D})$ on the space L^2_w on the basis $\mathcal{Y}^{1/w}_s$.

In the next section we propose some new boundary integral operators. They are defined as convolution operators with kernels defined on $\mathbb{D}$, conceived to exhibit singular behavior near the edge, resembling that of the kernels of the inverse integral operators derived for the segment in $\mathbb{R}^2$. Their closed-form expressions have similarities with those involved in the method of images, used to derive half-space Green's functions. Although similar, they are not directly related. The use of mirror points in the developments presented in the next section are due to convenient transformations of the unit disk screen object into another one whose interior is not void, in this case, the unit sphere for convenience. These transformations show how the disk can be seen as a sphere collapsed into a two-sided screen by a limit process, making the exterior domain lose its Lipschitz-regularity.

3.2. Some boundary integral operators. Using the known behavior on ρ of the disk basis functions, we propose new integral kernels defined on $\mathbb{D}$. Two of these kernels have the same behavior of the kernels of the inverse operators in the case of the segment in $\mathbb{R}^2$ along the radius (on the ρ direction).

Definition 3.10 (new integral kernels for the disk). *Let us define the following two weakly singular integral kernels for* $(\mathbf{x},\mathbf{y}) \in \mathbb{D}\times\mathbb{D}$ *with* $\mathbf{x}\neq\mathbf{y}$*:*

$$K^{ws}_s(\mathbf{x},\mathbf{y}) = \sum_{l=0}^{\infty} \sum_{\substack{m=-l \\ l+m\ even}}^{l} \zeta_l y_l^m(\mathbf{y})\overline{y_l^m(\mathbf{x})} \quad \text{and} \quad K^{ws}_{as}(\mathbf{x},\mathbf{y}) = \sum_{l=0}^{\infty} \sum_{\substack{m=-l \\ l+m\ odd}}^{l} \zeta_l y_l^m(\mathbf{y})\overline{y_l^m(\mathbf{x})}$$

with $\zeta_l = 2/(2l+1)$*. Similarly, let us define the following two hypersingular integral kernels for* $(\mathbf{x},\mathbf{y}) \in \mathbb{D}\times\mathbb{D}$ *with* $\mathbf{x}\neq\mathbf{y}$*:*

$$K^{hs}_s(\mathbf{x},\mathbf{y}) = -\sum_{l=0}^{\infty} \sum_{\substack{m=-l \\ l+m\ even}}^{l} \eta_l \frac{y_l^m(\mathbf{y})}{w(\mathbf{x})} \frac{\overline{y_l^m(\mathbf{x})}}{w(\mathbf{y})} \quad \text{and} \quad K^{hs}_{as}(\mathbf{x},\mathbf{y}) = -\sum_{l=0}^{\infty} \sum_{\substack{m=-l \\ l+m\ odd}}^{l} \eta_l \frac{y_l^m(\mathbf{y})}{w(\mathbf{x})} \frac{\overline{y_l^m(\mathbf{x})}}{w(\mathbf{y})}$$

with $\eta_l = 2l(l+1)/(2l+1)$*.*

The behavior on ρ of the proposed kernels K^{ws}_{as} and K^{hs}_s matches that of those derived for the segment in $\mathbb{R}^2$ in that they have same singularity near the edge. This becomes clear comparing the behavior on ρ described in Remark 3.5 with that of the kernels for the segment in (4). The coefficients of the series are chosen following [14, equations 3.2.30 and 3.2.31], which provides a tool for relating series expressions of the kernels to closed-form expressions.

Definition 3.11 (associated boundary integral operators). *For* $\mathbf{y}\in\mathbb{D}$ *we define the following boundary integral operators:*

$$\left(\mathcal{S}_s\lambda\right)(\mathbf{y}) = \int_{\mathbb{D}} K^{ws}_s(\mathbf{x},\mathbf{y})\lambda(\mathbf{x})d\mathbb{D}(\mathbf{x}), \quad \left(\mathcal{S}_{as}\varphi\right)(\mathbf{y}) = \int_{\mathbb{D}} K^{ws}_{as}(\mathbf{x},\mathbf{y})\varphi(\mathbf{x})d\mathbb{D}(\mathbf{x}),$$
$$\left(\mathcal{N}_s g\right)(\mathbf{y}) = \int_{\mathbb{D}} K^{hs}_s(\mathbf{x},\mathbf{y})g(\mathbf{x})d\mathbb{D}(\mathbf{x}), \quad \left(\mathcal{N}_{as}\mu\right)(\mathbf{y}) = \int_{\mathbb{D}} K^{hs}_{as}(\mathbf{x},\mathbf{y})\mu(\mathbf{x})d\mathbb{D}(\mathbf{x}).$$

PROPOSITION 3.12 (mapping properties of the new boundary integral operators). *The boundary integral operators from Definition* 3.11 *have the following mapping properties:*

$$\mathcal{S}_s \frac{y_l^m}{w} = \frac{\zeta_l}{2} y_l^m \quad \text{and} \quad \mathcal{N}_s y_l^m = -\frac{\eta_l}{2}\frac{y_l^m}{w} \quad \text{for } l+m \text{ even},$$
$$\mathcal{S}_{as} \frac{y_l^m}{w} = \frac{\zeta_l}{2} y_l^m \quad \text{and} \quad \mathcal{N}_{as} y_l^m = -\frac{\eta_l}{2}\frac{y_l^m}{w} \text{ for } l+m \text{ odd}.$$

Proof. Let us analyze the first case.

$$\left(\mathcal{S}_s \frac{y_l^m}{w}\right)(\mathbf{y}) = \sum_{l'=0}^{\infty} \sum_{\substack{m'=-l' \\ l'+m' \text{ even}}}^{l'} \zeta_l \int_{\mathbb{D}} y_{l'}^{m'}(\mathbf{y}) \overline{y_{l'}^{m'}}(\mathbf{x}) \frac{y_l^m(\mathbf{x})}{w(\mathbf{x})} d\mathbb{D}(\mathbf{x}).$$

Using the orthogonality relation of Proposition 3.3 the desired results follow straightforwardly. The same procedure proves the other three cases. ∎

PROPOSITION 3.13 (Calderón-type identities for new boundary integral operators). *The following operator composition identities hold for the boundary integral operators from Definition* 3.11*:*

$$-\mathcal{N}_s \circ \mathcal{S}_s \lambda = \frac{1}{4}\left(\mathbb{I} + \frac{1}{w}\mathcal{S}_s\left(\frac{1}{w}\mathcal{S}_s\lambda\right)\right), \quad -\mathcal{N}_{as} \circ \mathcal{S}_{as}\varphi = \frac{1}{4}\left(\mathbb{I} + \frac{1}{w}\mathcal{S}_{as}\left(\frac{1}{w}\mathcal{S}_{as}\varphi\right)\right),$$
$$-\mathcal{S}_s \circ \mathcal{N}_s g = \frac{1}{4}\left(\mathbb{I} + \mathcal{S}_s\left(\frac{1}{w}\mathcal{S}_s\left(\frac{g}{w}\right)\right)\right), \quad -\mathcal{S}_{as} \circ \mathcal{N}_{as}\mu = \frac{1}{4}\left(\mathbb{I} + \mathcal{S}_{as}\left(\frac{1}{w}\mathcal{S}_{as}\left(\frac{\mu}{w}\right)\right)\right).$$

Proof. Let us prove the first identity for $\mathcal{N}_s \circ \mathcal{S}_s$. Using Proposition 3.12 it's easy to see that

$$-\left(\mathcal{N}_s \circ \mathcal{S}_s\right)\lambda = \frac{1}{4}\sum_{l=0}^{\infty} \sum_{\substack{m=-l \\ l+m \text{ even}}}^{l} \zeta_l \eta_l \lambda_l^m \frac{y_l^m}{w} = \sum_{l=0}^{\infty} \sum_{\substack{m=-l \\ l+m \text{ even}}}^{l} \frac{l(l+1)}{(2l+1)^2} \lambda_l^m \frac{y_l^m}{w}.$$

This expression can be separated as

$$\sum_{l=0}^{\infty} \sum_{\substack{m=-l \\ l+m \text{ even}}}^{l} \frac{l(l+1)}{(2l+1)^2} \lambda_l^m \frac{y_l^m}{w} = \sum_{l=0}^{\infty} \sum_{\substack{m=-l \\ l+m \text{ even}}}^{l} \lambda_l^m \frac{y_l^m}{w} - \sum_{l=0}^{\infty} \sum_{\substack{m=-l \\ l+m \text{ even}}}^{l} \frac{3l^2+3l+1}{(2l+1)^2} \lambda_l^m \frac{y_l^m}{w}$$
$$= \lambda - 3\sum_{l=0}^{\infty} \sum_{\substack{m=-l \\ l+m \text{ even}}}^{l} \frac{l(l+1)}{(2l+1)^2} \lambda_l^m \frac{y_l^m}{w} - \sum_{l=0}^{\infty} \sum_{\substack{m=-l \\ l+m \text{ even}}}^{l} \frac{\lambda_l^m}{(2l+1)^2} \frac{y_l^m}{w}$$
$$\Rightarrow -4\left(\mathcal{N}_s \circ \mathcal{S}_s\right)\lambda = \lambda - \sum_{l=0}^{\infty} \sum_{\substack{m=-l \\ l+m \text{ even}}}^{l} \frac{1}{(2l+1)^2} \lambda_l^m \frac{y_l^m}{w}. \tag{5}$$

The last term of the equation is easy to compose using operator $\mathcal{S}_s$. It is easy to see that

$$\frac{1}{w}\mathcal{S}_s\left(\frac{1}{w}\mathcal{S}_s\lambda\right) = \sum_{l=0}^{\infty} \sum_{\substack{m=-l \\ l+m \text{ even}}}^{l} \frac{1}{(2l+1)^2} \lambda_l^m \frac{y_l^m}{w},$$

which proves the first case. The case for $\mathcal{N}_{as} \circ \mathcal{S}_{as}$ is done in the same way but by summing over $l+m$ odd pairs.

In the case of $\mathcal{S}_s \circ \mathcal{N}_s$,

$$-\left(\mathcal{S}_s \circ \mathcal{N}_s\right) g = \sum_{0 \leq l} \sum_{\substack{-l \leq m \leq l \\ l+m \text{ even}}} \frac{l(l+1)}{(2l+1)^2} g_l^m y_l^m.$$

Using again Proposition 3.3 it is easy to see that

$$\mathcal{S}_s\left(\frac{1}{w}\mathcal{S}_s\left(\frac{g}{w}\right)\right) = \sum_{0 \leq l} \sum_{\substack{-l \leq m \leq l \\ l+m \text{ even}}} \frac{1}{(2l+1)^2} g_l^m y_l^m.$$

The procedure of the proof is then exactly as the previous two cases replacing y_l^m/w with y_l^m. The case for $\mathcal{S}_{as} \circ \mathcal{N}_{as}$ is done in the same way but summing over $l+m$ odd pairs. ∎

3.3. Variational expressions. In this section we are interested in finding closed-form variational expressions for the new boundary integral operators from Definition 3.11. These variational expressions are needed for the computation of the Galerkin matrices required by the boundary element methods. The following two theorems provide the desired closed-form variational expressions for the new integral operators defined in series expansions.

THEOREM 3.14 (explicit and closed form of the weakly singular integral kernels). *The weakly singular integral operators from Definition* 3.11 *have the following explicit and closed-form variational expressions:*

$$\left\langle \mathcal{S}_s \lambda \,,\, \lambda^t \right\rangle_{\mathbb{D}} = \int_{\mathbb{D}} \int_{\mathbb{D}} \left(G(\mathbf{x}^+, \mathbf{y}^+) + G(\mathbf{x}^-, \mathbf{y}^+) \right) \lambda(\mathbf{x}) \lambda^t(\mathbf{y}) d\mathbb{D}(\mathbf{x}) d\mathbb{D}(\mathbf{y}), \tag{6}$$

$$\left\langle \mathcal{S}_{as} \varphi \,,\, \varphi^t \right\rangle_{\mathbb{D}} = \int_{\mathbb{D}} \int_{\mathbb{D}} \left(G(\mathbf{x}^+, \mathbf{y}^+) - G(\mathbf{x}^-, \mathbf{y}^+) \right) \varphi(\mathbf{x}) \varphi^t(\mathbf{y}) d\mathbb{D}(\mathbf{x}) d\mathbb{D}(\mathbf{y}). \tag{7}$$

Proof. Let us first consider the case of K_s^{ws}. Let us consider a projection $T : \mathbb{S} \to \mathbb{D}$ taking points on the sphere to their vertical projections on the disk ($\mathbf{y} = T\mathbf{y}^+ = T\mathbf{y}^- \in \mathbb{D}$), to be used in integration by substitution. The application of $\mathcal{S}_s$ to a function λ defined on the disk yields, for $\mathbf{y} \in \mathbb{D}$,

$$\begin{aligned}
(\mathcal{S}_s \lambda)(\mathbf{y}) &= \int_{\mathbb{D}} K_s^{ws}(\mathbf{x}, \mathbf{y}) \lambda(\mathbf{x}) d\mathbb{D}(\mathbf{x}) \\
&= \int_{\mathbb{S}^+} \sum_{l=0}^{\infty} \sum_{\substack{m=-l \\ l+m \text{ even}}}^{l} \zeta_l \overline{y_l^m(T\mathbf{x})} y_l^m(T\mathbf{y}^+) \lambda(T\mathbf{x}) |\cos\theta_{\mathbf{x}}| d\mathbb{S}^+(\mathbf{x}).
\end{aligned}$$

Let us define $\lambda^+ = \lambda \circ T$ over $\mathbb{S}^+$, so that the application of $\mathcal{S}_s$ can be fully pulled to the upper sphere,

$$\left(\mathcal{S}_s \lambda\right)(\mathbf{y}) = \int_{\mathbb{S}^+} \sum_{l=0}^{\infty} \sum_{\substack{m=-l \\ l+m \text{ even}}}^{l} \zeta_l \overline{Y_l^m(\mathbf{x})} Y_l^m(\mathbf{y}^+) \lambda^+(\mathbf{x}) |\cos\theta_{\mathbf{x}}| d\mathbb{S}^+(\mathbf{x}).$$

Let us now define $\widetilde{\lambda^+}$ as the mirror reflection over $\mathbb{S}^-$, so that it is an even function of x_3, i.e., $\widetilde{\lambda^+}(\mathbf{x}^+) = \widetilde{\lambda^+}(\mathbf{x}^-)$. Because $\overline{Y_l^m}(\mathbf{x})$ (for $l+m$ even), $|\cos\theta_{\mathbf{x}}|$, and $\widetilde{\lambda^+}(\mathbf{x})$ are even functions of x_3, the integration can be computed on the whole sphere as

$$(\mathcal{S}_s\lambda)(\mathbf{y}) = \frac{1}{2}\int_{\mathbb{S}} \sum_{l=0}^{\infty} \sum_{\substack{m=-l \\ l+m \text{ even}}}^{l} \zeta_l \overline{Y_l^m(\mathbf{x})} Y_l^m(\mathbf{y}^+) \widetilde{\lambda^+}(\mathbf{x}) |\cos\theta_{\mathbf{x}}| d\mathbb{S}(\mathbf{x}). \tag{8}$$

Also, for the rest of the l, m pairs, when $l+m$ is odd, Y_l^m is odd, so that the integrand is also odd, and thus

$$l+m \text{ odd } \Rightarrow \int_{\mathbb{S}} \overline{Y_l^m(\mathbf{x})} Y_l^m(\mathbf{y}^+) \widetilde{\lambda^+}(\mathbf{x}) |\cos\theta_{\mathbf{x}}| d\mathbb{S}(\mathbf{x}) = 0.$$

Now these terms can be added to (8), so that the sum has all the l, m pairs:

$$(\mathcal{S}_s\lambda)(\mathbf{y}) = \frac{1}{2}\int_{\mathbb{S}} \sum_{0=l}^{\infty} \sum_{m=-l}^{l} \zeta_l \overline{Y_l^m(\mathbf{x})} Y_l^m(\mathbf{y}^+) \widetilde{\lambda^+}(\mathbf{x}) |\cos\theta_{\mathbf{x}}| d\mathbb{S}(\mathbf{x}). \tag{9}$$

By construction $\zeta_l/2 = 1/(2l+1)$ for which [14, equation 3.2.30] allows us to rewrite (9).

$$\begin{aligned}
(\mathcal{S}_s\lambda)(\mathbf{y}) &= \int_{\mathbb{S}} G(\mathbf{x},\mathbf{y}^+) \widetilde{\lambda^+}(\mathbf{x}) |\cos\theta_{\mathbf{x}}| d\mathbb{S}(\mathbf{x}) \\
&= \int_{\mathbb{S}^+} G(\mathbf{x},\mathbf{y}^+) \widetilde{\lambda^+}(\mathbf{x}) |\cos\theta_{\mathbf{x}}| d\mathbb{S}^+(\mathbf{x}) + \int_{\mathbb{S}^-} G(\mathbf{x},\mathbf{y}^+) \widetilde{\lambda^+}(\mathbf{x}) |\cos\theta_{\mathbf{x}}| d\mathbb{S}^-(\mathbf{x}) \\
&= \int_{\mathbb{D}} G(\mathbf{x}^+,\mathbf{y}^+) \lambda(\mathbf{x}) d\mathbb{D}(\mathbf{x}) + \int_{\mathbb{D}} G(\mathbf{x}^-,\mathbf{y}^+) \lambda(\mathbf{x}) d\mathbb{D}(\mathbf{x}) \\
&= \int_{\mathbb{D}} \frac{1}{4\pi} \left(\frac{1}{\|\mathbf{x}^+ - \mathbf{y}^+\|} + \frac{1}{\|\mathbf{x}^- - \mathbf{y}^+\|} \right) \lambda(\mathbf{x}) d\mathbb{D}(\mathbf{x}).
\end{aligned}$$

This proves the identity (6) of the theorem.

The proof for $\mathcal{S}_{as}$ can be deduced using the same argument with some modifications. Starting with the series definitions for $\mathcal{S}_{as}\varphi$, a function $\varphi^+ = \varphi \circ T$ is defined to pull the integral over $\mathbb{S}^+$. Defining $\widetilde{\varphi^+}$ now as the odd mirror reflection, the same key properties are obtained: (1) the integrand becomes even and thus it can be transformed into an integral over $\mathbb{S}$, and (2) the complementary l, m pairs (the even ones) integrate as zero and can be added to complete the series. Once the expression of the integral kernel for the sphere is recognizable from [14, equation 3.2.20], it can be replaced and the integral then pulled back to the disk. Because $\widetilde{\varphi^+}$ is odd, the minus sign appears, naturally differentiating this case from the previous one. ∎

THEOREM 3.15 (explicit and closed variational form of the hypersingular integral kernels). *The bilinear form induced by the hypersingular boundary integral operator $\mathcal{N}_{as}$ admits the following explicit and closed-form variational expression:*

$$\left\langle -\mathcal{N}_{as}\mu\,,\,\mu^t \right\rangle_{\mathbb{D}} = \left\langle \mathcal{S}_s \overrightarrow{curl}_{\mathbb{D}}\mu, \overrightarrow{curl}_{\mathbb{D}}\mu^t \right\rangle_{\mathbb{D}} + \left\langle \mathcal{S}_{as}\left(\frac{1}{w}\frac{\partial\mu}{\partial\phi_{\mathbf{x}}}\right), \frac{1}{w}\frac{\partial\mu^t}{\partial\phi_{\mathbf{y}}} \right\rangle_{\mathbb{D}}. \tag{10}$$

Similarly, the bilinear form induced by the hypersingular boundary integral operator $\mathcal{N}_s$ admits the following explicit closed-form variational expression:

$$\left\langle -\mathcal{N}_s g\,,\,g^t \right\rangle_{\mathbb{D}} = \left\langle \mathcal{S}_{as} \overrightarrow{curl}_{\mathbb{D}}g, \overrightarrow{curl}_{\mathbb{D}}g^t \right\rangle_{\mathbb{D}} + \left\langle \mathcal{S}_s\left(\frac{1}{w}\frac{\partial g}{\partial\phi_{\mathbf{x}}}\right), \frac{1}{w}\frac{\partial g^t}{\partial\phi_{\mathbf{y}}} \right\rangle_{\mathbb{D}}. \tag{11}$$

Proof. Let us prove identity (10); identity (11) can be deduced analogously. The bilinear form induced by $\mathcal{N}_{as}$ is written as

$$\left\langle -\mathcal{N}_{as}\mu\,,\,\mu^t\right\rangle_{\mathbb{D}} = \int_{\mathbb{D}}\int_{\mathbb{D}}\sum_{l=0}^{\infty}\sum_{\substack{m=-l\\ l+m\ \text{odd}}}^{l}\eta_l\frac{\overline{y_l^m(\mathbf{x})}}{w(\mathbf{x})}\frac{y_l^m(\mathbf{y})}{w(\mathbf{y})}\mu(\mathbf{x})\overline{\mu^t}(\mathbf{y})d\mathbb{D}(\mathbf{x})d\mathbb{D}(\mathbf{y}).$$

Let us define $T:\mathbb{S}\to\mathbb{D}$ as the vertical projection of points from the sphere onto the disk, and the following odd functions are defined for points $\mathbf{x},\mathbf{y}$ over $\mathbb{S}$:

$$\tilde{\mu}(\mathbf{x}) = \begin{cases} \mu(T\mathbf{x}) & \text{if } \mathbf{x}\in\mathbb{S}^+,\\ -\mu(T\mathbf{x}) & \text{if } \mathbf{x}\in\mathbb{S}^-,\end{cases} \quad\text{and } \tilde{\mu}^t(\mathbf{y}) = \begin{cases} \mu^t(T\mathbf{y}) & \text{if } \mathbf{y}\in\mathbb{S}^+,\\ -\mu^t(T\mathbf{y}) & \text{if } \mathbf{y}\in\mathbb{S}^-.\end{cases}$$

Defined like this, we identify $\overline{Y_l^m(\mathbf{x})}\tilde{\mu}(\mathbf{x})$ and $Y_l^m(\mathbf{y})\overline{\tilde{\mu}^t}(\mathbf{y})$ as even functions for $l+m$ odd, and as odd functions for $l+m$ even. Thus, we can rewrite the bilinear form as

$$\begin{aligned}\left\langle -\mathcal{N}_{as}\mu\,,\mu^t\right\rangle_{\mathbb{D}} &= \frac{1}{2}\int_{\mathbb{S}}\int_{\mathbb{S}}\sum_{l=0}^{\infty}\sum_{m=-l}^{l}\frac{\eta_l}{2}\overline{Y_l^m(\mathbf{x})}Y_l^m(\mathbf{y})\tilde{\mu}(\mathbf{x})\overline{\tilde{\mu}^t}(\mathbf{y})d\mathbb{S}(\mathbf{x})d\mathbb{S}(\mathbf{y})\\ &= \frac{1}{2}\int_{\mathbb{S}}\int_{\mathbb{S}}\frac{\partial^2 G}{\partial_{n_{\mathbf{x}}}\partial_{n_{\mathbf{y}}}}(\mathbf{x},\mathbf{y})\tilde{\mu}(\mathbf{x})\overline{\tilde{\mu}^t}(\mathbf{y})d\mathbb{S}(\mathbf{x})d\mathbb{S}(\mathbf{y}) \quad [14,\text{ equation 3.2.31}]\\ &= \frac{1}{2}\int_{\mathbb{S}}\int_{\mathbb{S}}G(\mathbf{x},\mathbf{y})\left(\overrightarrow{\operatorname{curl}}_{\mathbb{S}}\tilde{\mu}(\mathbf{x}),\overrightarrow{\operatorname{curl}}_{\mathbb{S}}\tilde{\mu}^t(\mathbf{y})\right)d\mathbb{S}(\mathbf{x})d\mathbb{S}(\mathbf{y})\,[14,\text{ theorem 3.3.2}].\end{aligned}$$

Developing the inner product, we can rewrite again the previous expression as

(12)

$$\begin{aligned}&\left\langle -\mathcal{N}_{as}\mu\,,\,\mu^t\right\rangle_{\mathbb{D}}\\ &= \frac{1}{2}\int_{\mathbb{S}}\int_{\mathbb{S}}G(\mathbf{x},\mathbf{y})\left[\cos\left(\phi_{\mathbf{x}}-\phi_{\mathbf{y}}\right)\left(\frac{\partial\tilde{\mu}(\mathbf{x})}{\partial\theta_{\mathbf{x}}}\frac{\partial\overline{\tilde{\mu}^t}(\mathbf{y})}{\partial\theta_{\mathbf{y}}}+\frac{\cos\theta_{\mathbf{x}}\cos\theta_{\mathbf{y}}}{\sin\theta_{\mathbf{x}}\sin\theta_{\mathbf{y}}}\frac{\partial\tilde{\mu}(\mathbf{x})}{\partial\phi_{\mathbf{x}}}\frac{\partial\overline{\tilde{\mu}^t}(\mathbf{y})}{\partial\phi_{\mathbf{y}}}\right)\right.\\ &\quad\left.+\sin\left(\phi_{\mathbf{x}}-\phi_{\mathbf{y}}\right)\left(\frac{\cos\theta_{\mathbf{y}}}{\sin\theta_{\mathbf{y}}}\frac{\partial\tilde{\mu}(\mathbf{x})}{\partial\theta_{\mathbf{x}}}\frac{\partial\overline{\tilde{\mu}^t}(\mathbf{y})}{\partial\phi_{\mathbf{y}}}-\frac{\cos\theta_{\mathbf{x}}}{\sin\theta_{\mathbf{x}}}\frac{\partial\tilde{\mu}(\mathbf{x})}{\partial\phi_{\mathbf{x}}}\frac{\partial\overline{\tilde{\mu}^t}(\mathbf{y})}{\partial\theta_{\mathbf{y}}}\right)\right]\cos\theta_{\mathbf{x}}\cos\theta_{\mathbf{y}}d\mathbb{S}(\mathbf{x})d\mathbb{S}(\mathbf{y})\\ &\quad+\frac{1}{2}\int_{\mathbb{S}}\int_{\mathbb{S}}G(\mathbf{x},\mathbf{y})\frac{\partial\tilde{\mu}(\mathbf{x})}{\partial\phi_{\mathbf{x}}}\frac{\partial\overline{\tilde{\mu}^t}(\mathbf{y})}{\partial\phi_{\mathbf{y}}}d\mathbb{S}(\mathbf{x})d\mathbb{S}(\mathbf{y}).\end{aligned}$$

Let us focus on the second integral. The integral operator linked to the Laplace Green's function can be rewritten using series expansions as [14, equation 3.2.30]

$$\begin{aligned}&\frac{1}{2}\int_{\mathbb{S}}\int_{\mathbb{S}}G(\mathbf{x},\mathbf{y})\frac{\partial\tilde{\mu}(\mathbf{x})}{\partial\phi_{\mathbf{x}}}\frac{\partial\overline{\tilde{\mu}^t}(\mathbf{y})}{\partial\phi_{\mathbf{y}}}d\mathbb{S}(\mathbf{x})d\mathbb{S}(\mathbf{y})\\ &\quad=\frac{1}{2}\int_{\mathbb{S}}\int_{\mathbb{S}}\sum_{l=0}^{\infty}\sum_{m=-l}^{l}\frac{\zeta_l}{2}\overline{Y_l^m(\mathbf{x})}Y_l^m(\mathbf{y})\frac{\partial\tilde{\mu}(\mathbf{x})}{\partial\phi_{\mathbf{x}}}\frac{\partial\overline{\tilde{\mu}^t}(\mathbf{y})}{\partial\phi_{\mathbf{y}}}d\mathbb{S}(\mathbf{x})d\mathbb{S}(\mathbf{y}).\end{aligned}$$

Since $\tilde{\mu}$ and $\overline{\tilde{\mu}^t}$ are odd functions we can write

$$\begin{aligned}&\frac{1}{2}\int_{\mathbb{S}}\int_{\mathbb{S}}G(\mathbf{x},\mathbf{y})\frac{\partial\tilde{\mu}(\mathbf{x})}{\partial\phi_{\mathbf{x}}}\frac{\partial\overline{\tilde{\mu}^t}(\mathbf{y})}{\partial\phi_{\mathbf{y}}}d\mathbb{S}(\mathbf{x})d\mathbb{S}(\mathbf{y})\\ &\quad=\frac{1}{2}\int_{\mathbb{S}}\int_{\mathbb{S}}\sum_{l=0}^{\infty}\sum_{\substack{m=-l\\ l+m\ \text{odd}}}^{l}\frac{\zeta_l}{2}\overline{Y_l^m(\mathbf{x})}Y_l^m(\mathbf{y})\frac{\partial\tilde{\mu}(\mathbf{x})}{\partial\phi_{\mathbf{x}}}\frac{\partial\overline{\tilde{\mu}^t}(\mathbf{y})}{\partial\phi_{\mathbf{y}}}d\mathbb{S}(\mathbf{x})d\mathbb{S}(\mathbf{y})\end{aligned}$$

$$= \int_{\mathbb{S}^+}\int_{\mathbb{S}^+} \sum_{l=0}^{\infty} \sum_{\substack{m=-l \\ l+m \text{ odd}}}^{l} \zeta_l \overline{Y_l^m(\mathbf{x})} Y_l^m(\mathbf{y}) \frac{\partial \tilde{\mu}(\mathbf{x})}{\partial \phi_{\mathbf{x}}} \frac{\partial \overline{\tilde{\mu}^t}(\mathbf{y})}{\partial \phi_{\mathbf{y}}} d\mathbb{S}^+(\mathbf{x}) d\mathbb{S}^+(\mathbf{y})$$

$$= \int_{\mathbb{D}}\int_{\mathbb{D}} \sum_{l=0}^{\infty} \sum_{\substack{m=-l \\ l+m \text{ odd}}}^{l} \zeta_l \frac{\overline{y_l^m(\mathbf{x})}}{w(\mathbf{x})} \frac{y_l^m(\mathbf{y})}{w(\mathbf{y})} \frac{\partial \mu(\mathbf{x})}{\partial \phi_{\mathbf{x}}} \frac{\partial \overline{\mu^t}(\mathbf{y})}{\partial \phi_{\mathbf{y}}} d\mathbb{D}(\mathbf{x}) d\mathbb{D}(\mathbf{y})$$

$$= \left\langle \mathcal{S}_{as}\left(\frac{1}{w}\frac{\partial \mu}{\partial \phi_{\mathbf{x}}}\right), \frac{1}{w}\frac{\partial \mu^t}{\partial \phi_{\mathbf{y}}} \right\rangle_{\mathbb{D}},$$

thus providing the desired result for the second integration in (12).

Let us now address the first integral. Let us first note that the following functions are even with respect to the plane $x_3 = 0$:

$$\frac{\partial \tilde{\mu}}{\partial \theta_{\mathbf{x}}}(\mathbf{x}),\ \frac{\partial \tilde{\mu}^t}{\partial \theta_{\mathbf{y}}}(\mathbf{y}),\ \frac{\cos\theta_{\mathbf{x}}}{\sin\theta_{\mathbf{x}}}\frac{\partial \tilde{\mu}}{\partial \phi_{\mathbf{x}}}(\mathbf{x}),\ \text{ and }\ \frac{\cos\theta_{\mathbf{y}}}{\sin\theta_{\mathbf{y}}}\frac{\partial \tilde{\mu}^t}{\partial \phi_{\mathbf{y}}}(\mathbf{y});$$

thus we can rewrite the second integral in (12), eliminating the terms for $l+m$ odd, as

$$\frac{1}{2}\int_{\mathbb{S}}\int_{\mathbb{S}} \sum_{l=0}^{\infty} \sum_{\substack{m=-l \\ l+m \text{ even}}}^{l} \frac{\zeta_l}{2} \overline{Y_l^m(\mathbf{x})} Y_l^m(\mathbf{y}) \left[\cos(\phi_{\mathbf{x}} - \phi_{\mathbf{y}}) \left(\frac{\partial \tilde{\mu}(\mathbf{x})}{\partial \theta_{\mathbf{x}}} \frac{\partial \overline{\tilde{\mu}^t}(\mathbf{y})}{\partial \theta_{\mathbf{y}}} + \frac{\cos\theta_{\mathbf{x}}\cos\theta_{\mathbf{y}}}{\sin\theta_{\mathbf{x}}\sin\theta_{\mathbf{y}}} \frac{\partial \tilde{\mu}(\mathbf{x})}{\partial \phi_{\mathbf{x}}} \frac{\partial \overline{\tilde{\mu}^t}(\mathbf{y})}{\partial \phi_{\mathbf{y}}}\right)\right.$$
$$\left. + \sin(\phi_{\mathbf{x}} - \phi_{\mathbf{y}}) \left(\frac{\cos\theta_{\mathbf{y}}}{\sin\theta_{\mathbf{y}}} \frac{\partial \tilde{\mu}(\mathbf{x})}{\partial \theta_{\mathbf{x}}} \frac{\partial \overline{\tilde{\mu}^t}(\mathbf{y})}{\partial \phi_{\mathbf{y}}} - \frac{\cos\theta_{\mathbf{x}}}{\sin\theta_{\mathbf{x}}} \frac{\partial \tilde{\mu}(\mathbf{x})}{\partial \phi_{\mathbf{x}}} \frac{\partial \overline{\tilde{\mu}^t}(\mathbf{y})}{\partial \theta_{\mathbf{y}}}\right)\right] \cos\theta_{\mathbf{x}} \cos\theta_{\mathbf{y}} d\mathbb{S}(\mathbf{x}) d\mathbb{S}(\mathbf{y}).$$

Using the same procedure as before for writing sphere integrals of even functions as integrals on $\mathbb{S}^+$ and on $\mathbb{D}$ with a change of variables we find the desired expression for the first integral identifying

$$\left(\overrightarrow{\operatorname{curl}}_{\mathbb{D}}\tilde{\mu}(\mathbf{x}), \overrightarrow{\operatorname{curl}}_{\mathbb{D}}\tilde{\mu}^t(\mathbf{y})\right) = \cos(\phi_{\mathbf{x}} - \phi_{\mathbf{y}}) \left(\frac{\partial \tilde{\mu}(\mathbf{x})}{\partial \rho_{\mathbf{x}}} \frac{\partial \overline{\tilde{\mu}^t}(\mathbf{y})}{\partial \rho_{\mathbf{y}}} + \frac{1}{\rho_{\mathbf{x}}\rho_{\mathbf{y}}} \frac{\partial \tilde{\mu}(\mathbf{x})}{\partial \phi_{\mathbf{x}}} \frac{\partial \overline{\tilde{\mu}^t}(\mathbf{y})}{\partial \phi_{\mathbf{y}}}\right)$$
$$+ \sin(\phi_{\mathbf{x}} - \phi_{\mathbf{y}}) \left(\frac{\partial \tilde{\mu}(\mathbf{x})}{\partial \rho_{\mathbf{x}}} \frac{1}{\rho_{\mathbf{y}}} \frac{\partial \overline{\tilde{\mu}^t}(\mathbf{y})}{\partial \phi_{\mathbf{y}}} - \frac{1}{\rho_{\mathbf{x}}} \frac{\partial \tilde{\mu}(\mathbf{x})}{\partial \phi_{\mathbf{x}}} \frac{\partial \overline{\tilde{\mu}^t}(\mathbf{y})}{\partial \rho_{\mathbf{y}}}\right).$$

This proves (10) from the theorem. Equation (11) regarding $\mathcal{N}_s$ can be obtained with the same procedure using complementary parity and symmetry. ∎

DEFINITION 3.16 (associated norms). *It is convenient to use the developed variational forms to define norms to test the implementation in numerical experiments. Let us define the following norms using the variational forms associated with the boundary integral operators:*

$$\|\lambda\|_{\mathcal{S}_s} = \sqrt{\langle \mathcal{S}_s\lambda\,,\,\lambda\rangle_{\mathbb{D}}}, \quad \|\varphi\|_{\mathcal{S}_{as}} = \sqrt{\langle \mathcal{S}_{as}\varphi\,,\,\varphi\rangle_{\mathbb{D}}},$$
$$\|g\|_{\mathcal{N}_s} = \sqrt{\langle -\mathcal{N}_s g\,,\,g\rangle_{\mathbb{D}}}, \quad \|\mu\|_{\mathcal{N}_{as}} = \sqrt{-\langle \mathcal{N}_{as}\mu\,,\,\mu\rangle_{\mathbb{D}}}\,.$$

4. Numerical experiments. In this section we test the preconditioning capabilities of the proposed integral operators. We do so by first developing a domain discretization and boundary element spaces that satisfy the condition of having the same dimensions, as required by Theorem 2.1. We propose numerical methods to compute the associated Galerkin matrices and we test them through benchmarks using known solutions to the associated boundary integral equations. Finally, we test the preconditioning capabilities of the Galerkin matrices associated with the proposed boundary integral operators and an extension to screens other than the disk in $\mathbb{R}^3$.

4.1. Domain discretization. Let us consider a triangular mesh $\mathcal{T}_h$ of $\mathbb{D}$, made of N_T closed triangles (with K_i its ith triangle), N_E edges, and N_V vertices (with $\boldsymbol{r}_i$ its ith vertex), of which N_V^0 are interior. The new domain of integration $\mathbb{D}_h$, an approximation of $\mathbb{D}$, is then defined as $\mathbb{D}_h = \cup_{m=1}^{N_T} K_m$. We ask the mesh to comply with standard assumptions of conformity. Mesh $\mathcal{T}_h$ is used to define the basis functions of finite-dimensional subspaces of $H^{1/2}(\mathbb{D}_h)$ and $\widetilde{H}^{1/2}(\mathbb{D}_h)$. We need to consider dual meshes to define the basis functions of the finite-dimensional subspaces of $H^{-1/2}(\mathbb{D}_h)$ and $\widetilde{H}^{-1/2}(\mathbb{D}_h)$. These subspaces need different meshes in order to comply with one of the requisites demanded by Theorem 2.1, that is, that the finite-dimensional spaces used have the same number of dimensions. This is made clear during their construction and explained in following remarks.

Two dual meshes are constructed from $\mathcal{T}_h$. The first dual mesh $\tilde{\mathcal{T}}_h$ is constructed similarly as done in [18, section 2.2]: we consider the six subtriangles resulting from dividing each triangle using its medians (barycentric refinement). We consider the set of polygonal elements $\{L_i\}_{i=0}^{N_V}$, associated with the vertices of the mesh such that polygonal element L_i associated with $\boldsymbol{r}_i$ is the collection of subtriangles that have vertex i of the mesh as one of their own vertices. We consider a second dual mesh in order to develop appropriate elements for a subspace of $H^{-1/2}(\mathbb{D})$, dual to $\widetilde{H}^{1/2}(\mathbb{D})$ of functions zero on the border, and to comply with the requirement that finite subspaces have the same dimensions. The second dual mesh $\tilde{\mathcal{T}}_h^0$ uses a different subdivision of the triangles on the border of $\mathbb{D}_h$: the ones with two vertices over $\partial\mathbb{D}_h$ are not subdivided and are considered proper subtriangles, while the ones with one vertex over $\partial\mathbb{D}_h$ are divided into two subtriangles separated by the median associated with the vertex on the border $\partial\mathbb{D}_h$. The dual mesh $\tilde{\mathcal{T}}_h^0$ then considers the set polygonal elements $\{M_i\}_{i=0}^{N_V^0}$, associated with the internal vertices of the mesh such that element M_i associated with the internal vertex $\boldsymbol{r}_i$ is the collection of subtriangles (now produced differently) that have the internal vertex i of the mesh as one of their own vertices. Figure 1 shows specimens of the three meshes for $\mathbb{D}_h$ for a fixed h. Figure 2 illustrates the mesh construction process showing triangle subdivision at edge $\partial\mathbb{D}_h$.

In the presented new boundary integral operators related to the Laplace equation on the disk, the kernels involve projections of points from disk $\mathbb{D}$ onto the upper half-sphere $\mathbb{S}^+$ and onto the lower half-sphere $\mathbb{S}^-$. When performing numerical integrations over $\mathbb{D}_h$, advantage can be taken performing it instead over projected discretized domains $\mathbb{S}_h^+$ and $\mathbb{S}_h^-$, which can be constructed from $\mathbb{D}_h$ and vice versa using the

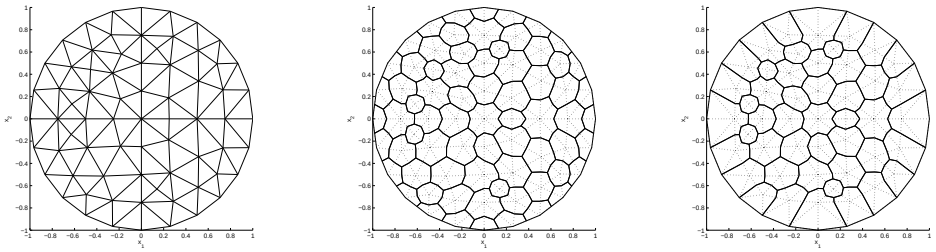

FIG. 1. *An example of a triangular mesh partition $\mathcal{T}_h$ of $\mathbb{D}_h$ for a given mean edge size h exhibiting its triangles $\{K_m\}_{m=1}^{N_T}$ (left), with the resulting dual meshes $\tilde{\mathcal{T}}_h$, exhibiting its polygonal components $\{L_i\}_{i=1}^{N_V}$ (center), and $\tilde{\mathcal{T}}_h^0$ exhibiting its polygonal components $\{M_i\}_{i=1}^{N_V^0}$ (right).*

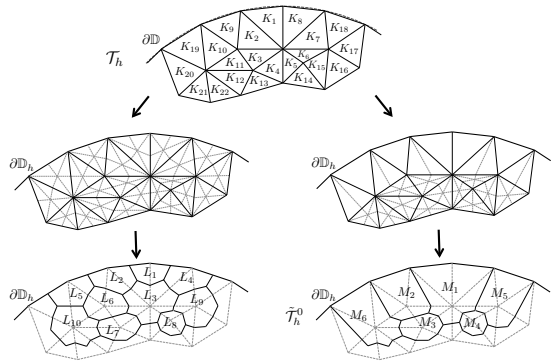

FIG. 2. *Detail of the subdivision of the triangles of mesh $\mathcal{T}_h$ near the border of $\partial\mathbb{D}_h$, showing the subdivision border triangles for the construction of $\tilde{\mathcal{T}}_h$ (left) and $\tilde{\mathcal{T}}_h^0$ (right).*

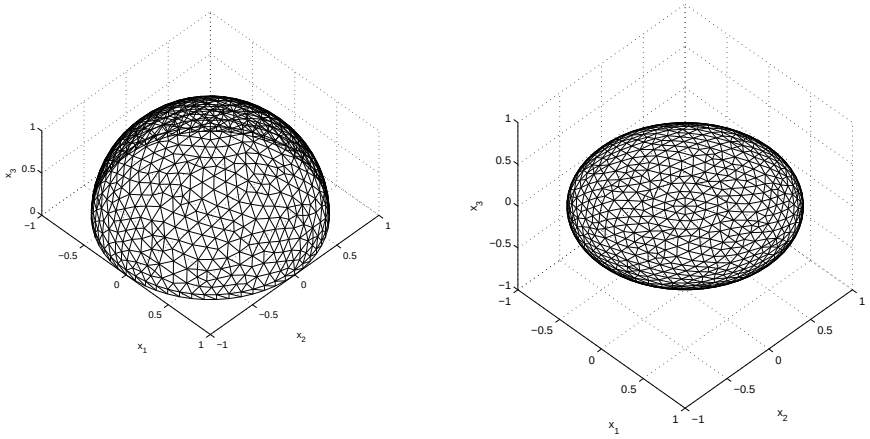

FIG. 3. *Example of a discretized domain $\mathbb{S}_h^+$ (left) and $\mathbb{D}_h$ (right), obtained as a vertical projection onto the plane.*

weight function w to compute the third component of the projected vertices. Figure 3 shows a discretized domain $\mathbb{S}_h^+$ and its projection $\mathbb{D}_h$ onto the plane. We use uniform meshes of $\mathbb{S}^+$ to produce vertically projected meshes of $\mathbb{D}_h$ and $\mathbb{S}_h^-$.

4.2. Boundary element spaces and computations. We employ the described meshes to build zeroth and first order piecewise polynomial boundary element spaces. We call $\mathbb{P}^n$ the space of bivariate polynomials of a degree less than or equal to n, and we then proceed to define boundary element spaces.

DEFINITION 4.1 (finite boundary element spaces). *Let us define the following finite boundary element spaces, piecewise polynomial on the polygonal shapes defined for the primal mesh $\mathcal{T}_h$ and the dual meshes $\tilde{\mathcal{T}}_h$ and $\tilde{\mathcal{T}}_h^0$:*

$$U_h = \left\{u_h \in C\left(\mathbb{D}_h\right) : \forall K_i \in \mathcal{T}_h \left(u_h|_{K_i} \in \mathbb{P}^1\right)\right\}, \quad U_h^0 = \left\{u_h \in U_h : u_h|_{\partial\mathbb{D}_h} = 0\right\},$$

$$V_h = \left\{v_h \in L^2(\mathbb{D}_h) : \forall L_i \in \tilde{\mathcal{T}}_h \left(v_h|_{L_i} \in \mathbb{P}^0\right)\right\}, \; V_h^0 = \left\{v_h \in L^2\left(\mathbb{D}_h\right) : \forall M_i \in \tilde{\mathcal{T}}_h^0 \left(v_h|_{M_i} \in \mathbb{P}^0\right)\right\}.$$

Remark 4.2 (dimension matching). Constructed like this, the defined finite-dimensional spaces are subspaces of the Sobolev trace spaces involved in the symmetric Dirichlet and antisymmetric Neumann problems, i.e.,

$$U_h \subset H^{1/2}(\mathbb{D}_h),\ U_h^0 \subset \widetilde{H}^{1/2}(\mathbb{D}_h),\ V_h \subset \widetilde{H}^{-1/2}(\mathbb{D}_h),\ \text{and } V_h^0 \subset H^{-1/2}(\mathbb{D}_h).$$

It is also noteworthy that $\dim(U_h) = \dim(V_h) = N_V$, and $\dim(U_h^0) = \dim(V_h^0) = N_V^0$.

DEFINITION 4.3 (basis functions). *We implicitly denote the standard zeroth order, piecewise constant, and first order pyramidal finite element basis functions (cf.* [16, section 4.1]*) for the previously defined finite-dimensional spaces through the following identities:*

$$span\Big(\{\chi_i\}_{i=1}^{N_V}\Big) = U_h,\ span\Big(\{\chi_i^0\}_{i=1}^{N_V^0}\Big) = U_h^0,\ span\Big(\{\kappa_i\}_{i=1}^{N_V}\Big) = V_h,\ span\Big(\{\kappa_i^0\}_{i=1}^{N_V^0}\Big) = V_h^0.$$

For piecewise affine functions χ_i or χ_i^0 we will denote their restriction to a triangle K_m as $\chi_i^{K_m}(\mathbf{x}) = a_i^m x_1 + b_i^m x_2 + c_i^m$. We write $K_m \ni \boldsymbol{r}_i$ to signify that $\boldsymbol{r}_i$ is one of the vertices of K_m.

In what follows we describe how to compute numerically the bilinear forms from Theorems 3.14 and 3.15 when evaluated at the basis functions of the different finite-dimensional spaces from Definition 4.1.

To compute the boundary element integrals we consider the subtriangles that compose triangles and polygonal elements defined for the primal mesh and for the dual meshes. Let k_i be a subtriangle belonging to a polygonal element from $\tilde{\mathcal{T}}_h$ or $\tilde{\mathcal{T}}_h^0$ or to a triangle from $\mathcal{T}_h$. We denote by k_i^+ and k_i^- the triangles resulting from projecting it onto the upper half-sphere $\mathbb{S}^+$ and onto the lower half-sphere $\mathbb{S}^-$, respectively. The unit vector normal to a subtriangle k_i is denoted by $\boldsymbol{n}^{k_i}$, and its components are indicated with subindices.

PROPOSITION 4.4 (computation of bilinear variational forms associated with $\mathcal{S}_s$ and $\mathcal{S}_{as}$). *The values of the bilinear forms associated with the weakly singular integral operators $\mathcal{S}_s$ and $\mathcal{S}_{as}$ for the piecewise constant basis functions are*

$$\langle \mathcal{S}_s \kappa_i\,,\, \kappa_j \rangle_{\mathbb{D}_h} = \int_{L_i}\int_{L_j} G\left(\boldsymbol{x}^+, \boldsymbol{y}^+\right) dL_i(\boldsymbol{x}) dL_j(\boldsymbol{y}) + \int_{L_i}\int_{L_j} G\left(\boldsymbol{x}^-, \boldsymbol{y}^+\right) dL_i(\boldsymbol{x}) dL_j(\boldsymbol{y}),$$

$$\left\langle \mathcal{S}_{as} \kappa_i^0\,,\, \kappa_j^0 \right\rangle_{\mathbb{D}_h} = \int_{M_i}\int_{M_j} G\big(\boldsymbol{x}^+, \boldsymbol{y}^+\big) dM_i(\boldsymbol{x}) dM_j(\boldsymbol{y}) - \int_{M_i}\int_{M_j} G\big(\boldsymbol{x}^-, \boldsymbol{y}^+\big) dM_i(\boldsymbol{x}) dM_j(\boldsymbol{y}).$$

DEFINITION 4.5 (approximation of elementary integrals over polygonal shapes). *We use the following approximations, signaled by $\approx$, for the integration of the Laplace Green's function with the projected arguments:*

$$\int_{L_i}\int_{L_j} G\left(\boldsymbol{x}^\pm, \boldsymbol{y}^+\right) dL_i(\boldsymbol{x}) dL_j(\boldsymbol{y}) \approx \sum_{k_m \subset L_i} \sum_{k_n \subset L_j} \left| \boldsymbol{n}_3^{k_m^\pm} \boldsymbol{n}_3^{k_n^+} \right| \int_{k_m^\pm}\int_{k_n^+} G\left(\boldsymbol{x}, \boldsymbol{y}\right) dk_m^\pm(\boldsymbol{x}) dk_n^+(\boldsymbol{y}),$$

$$\int_{M_i}\int_{M_j} G\left(\boldsymbol{x}^\pm, \boldsymbol{y}^+\right) dM_i(\boldsymbol{x}) dM_j(\boldsymbol{y}) \approx \sum_{k_m \subset M_i} \sum_{k_n \subset M_j} \left| \boldsymbol{n}_3^{k_m^\pm} \boldsymbol{n}_3^{k_n^+} \right| \int_{k_m^\pm}\int_{k_n^+} G\left(\boldsymbol{x}, \boldsymbol{y}\right) dk_m^\pm(\boldsymbol{x}) dk_n^+(\boldsymbol{y}).$$

The values of the bilinear forms associated with the hypersingular integral operators $\mathcal{N}_s$ and $\mathcal{N}_{as}$ (Theorem 3.15) for the piecewise affine basis functions are

$$\langle -\mathcal{N}_{as} \chi_i^0\,,\, \chi_j^0 \rangle_{\mathbb{D}} = \left\langle \mathcal{S}_s \overrightarrow{\mathrm{curl}}_{\mathbb{D}} \chi_i^0, \overrightarrow{\mathrm{curl}} \chi_j^0 \right\rangle_{\mathbb{D}} + \left\langle \mathcal{S}_{as} \left(\frac{1}{w} \frac{\partial \chi_i^0}{\partial \phi_{\mathbf{x}}} \right), \frac{1}{w} \frac{\partial \chi_j^0}{\partial \phi_{\mathbf{y}}} \right\rangle_{\mathbb{D}}, \tag{13}$$

$$\langle -\mathcal{N}_{s} \chi_i\,,\, \chi_j \rangle_{\mathbb{D}} = \left\langle \mathcal{S}_{as} \overrightarrow{\mathrm{curl}}_{\mathbb{D}} \chi_i, \overrightarrow{\mathrm{curl}} \chi_j \right\rangle_{\mathbb{D}} + \left\langle \mathcal{S}_{s} \left(\frac{1}{w} \frac{\partial \chi_i}{\partial \phi_{\mathbf{x}}} \right), \frac{1}{w} \frac{\partial \chi_j}{\partial \phi_{\mathbf{y}}} \right\rangle_{\mathbb{D}}. \tag{14}$$

DEFINITION 4.6 (approximation of elementary integrals for affine functions over triangles). *We approximate the integrals involved in* (13) *and* (14). *Let us first define the function* F *for points* $\mathbf{x}, \mathbf{y} \in \mathbb{D}$, *triangles* m *and* n, *and vertices* i *and* j:

$$F(\mathbf{x},\mathbf{y},m,n,i,j) = \frac{\left[\mathbf{x}\cdot\begin{pmatrix} b_i^m \\ -a_i^m \end{pmatrix}\right]\left[\mathbf{y}\cdot\begin{pmatrix} b_j^n \\ -a_j^n \end{pmatrix}\right]}{w(\mathbf{x})w(\mathbf{y})}. \tag{15}$$

The integrals involved in (13) *and* (14) *can be computed as*

$$\begin{aligned}
&\left\langle \mathcal{S}_{s/as}\overrightarrow{curl}_{\mathbb{D}}\chi_i^{K_m}, \overrightarrow{curl}\chi_j^{K_n}\right\rangle_{\mathbb{D}} \\
&\quad = \left(a_i^m a_j^n + b_i^m b_j^n\right)\int_{K_m}\int_{K_n}\left(G(\mathbf{x}^+,\mathbf{y}^+) \pm G(\mathbf{x}^-,\mathbf{y}^+)\right)dK_m(\mathbf{x})dK_n(\mathbf{y}), \\
&\left\langle \mathcal{S}_{s/as}\left(\frac{1}{w}\frac{\partial\chi_i^{K_m}}{\partial\phi_{\mathbf{x}}}\right), \frac{1}{w}\frac{\partial\chi_j^{K_n}}{\partial\phi_{\mathbf{y}}}\right\rangle_{\mathbb{D}} \\
&\quad = \int_{K_m}\int_{K_n}\left(G(\mathbf{x}^+,\mathbf{y}^+) \pm G(\mathbf{x}^-,\mathbf{y}^+)\right)F(\mathbf{x},\mathbf{y},m,n)dK_m(\mathbf{x})dK_n(\mathbf{y}) \\
&\quad \approx F(\boldsymbol{r}_c^m,\boldsymbol{r}_c^n,m,n,i,j)\int_{K_m}\int_{K_n}\left(G(\mathbf{x}^+,\mathbf{y}^+) \pm G(\mathbf{x}^-,\mathbf{y}^+)\right)dK_m(\mathbf{x})dK_n(\mathbf{y}),
\end{aligned}$$

where $\boldsymbol{r}_c^m$ *and* $\boldsymbol{r}_c^n$ *are the centroids of triangles* m *and* n. *The integral of the Laplace Green's functions with the projected arguments can be computed as before as*

$$\int_{K_m}\int_{K_n} G(\mathbf{x}^{\pm},\mathbf{y}^+)dK_m(\mathbf{x})dK_n(\mathbf{y}) \approx \left|\boldsymbol{n}_3^{K_m^{\pm}}\boldsymbol{n}_3^{K_n^+}\right|\int_{K_m^{\pm}}\int_{K_n^+} G(\mathbf{x},\mathbf{y})dK_m^{\pm}(\mathbf{x})dK_n^+(\mathbf{y}).$$

Remark 4.7 (kernel integration for pairs of triangles in $\mathbb{R}^3$). After approximating integration over the vertically projected triangles, elementary triangle integration, i.e., the integration of the Laplace Green's function G over any two triangles in $\mathbb{R}^3$, is computed as described in [3, sections D.12.3 and D.12.4], [1]: an analytical integration formula is used if the triangles intersect (if they share a vertex or an edge, or if they are the same triangle), and a numerical quadrature formula is used if they do not intersect.

DEFINITION 4.8 (Galerkin matrices associated with the new operators). *We define the Galerkin matrices associated with the bilinear forms described in this section. These matrices are used in the resolution of boundary integral equations associated with the proposed operators for testing purposes and later in preconditioning methods. Let us define the following matrices:*

$$\begin{aligned}
&\boldsymbol{S}_s^h[i,j] = \langle\mathcal{S}_s\kappa_i,\kappa_j\rangle_{\mathbb{D}_h}, \quad \boldsymbol{S}_{as}^h[i,j] = \langle\mathcal{S}_{as}\kappa_i^0,\kappa_j^0\rangle_{\mathbb{D}_h}, \\
&\boldsymbol{N}_s^h[i,j] = \langle\mathcal{N}_s\chi_i,\chi_j\rangle_{\mathbb{D}_h} + \alpha\langle\chi_i,1\rangle_{\mathbb{D}_h}\langle\chi_j,1\rangle_{\mathbb{D}_h}, \quad \boldsymbol{N}_{as}^h[i,j] = \langle\mathcal{N}_{as}\chi_i^0,\chi_j^0\rangle_{\mathbb{D}_h}.
\end{aligned}$$

The variational form associated with $\mathcal{N}_s$ *is augmented with a parameter* $\alpha \in \mathbb{R}^+$, *as shown in the expression of its Galerkin matrix, to eliminate the kernel space* $\{y_0^0\}$ *(cf. Proposition* 3.12*).*

Using Proposition 3.12, boundary integral equations with known exact solutions can be considered for each one of the four boundary integral operators on the disk. Approximations λ^h, μ^h, g^h, and φ^h can be computed with a finite-dimensional variational formulation using the described boundary element computations. Table 1 shows

TABLE 1
Four boundary integral equations associated with the four new boundary integral equations that will be used to test described numerical implementation.

Integral operator	Boundary integral operator	Exact solution	Numerical solution	Numerical error
$\mathcal{S}_s$	$\mathcal{S}_s\lambda = (1/3)y_1^1(\mathbf{x})$	$\lambda = y_1^1(\mathbf{x})w^{-1}(\mathbf{x})$	λ_h	$E_s^S = \|\lambda - \lambda_h\|_{\mathcal{S}_s}$
$\mathcal{S}_{as}$	$\mathcal{S}_{as}\varphi = (1/5)y_2^1(\mathbf{x})$	$\varphi = y_2^1(\mathbf{x})w^{-1}(\mathbf{x})$	φ_h	$E_{as}^S = \|\varphi - \varphi_h\|_{\mathcal{S}_{as}}$
$\mathcal{N}_s$	$\mathcal{N}_s g = -(2/3)y_1^1(\mathbf{x})w^{-1}(\mathbf{x})$	$g = y_1^1(\mathbf{x})$	g_h	$E_s^N = \|g - g_h\|_{\mathcal{N}_s}$
$\mathcal{N}_{as}$	$\mathcal{N}_{as}\mu = -(6/5)y_2^1(\mathbf{x})w^{-1}(\mathbf{x})$	$\mu = y_2^1(\mathbf{x})$	μ_h	$E_{as}^N = \|\mu - \mu_h\|_{\mathcal{N}_{as}}$

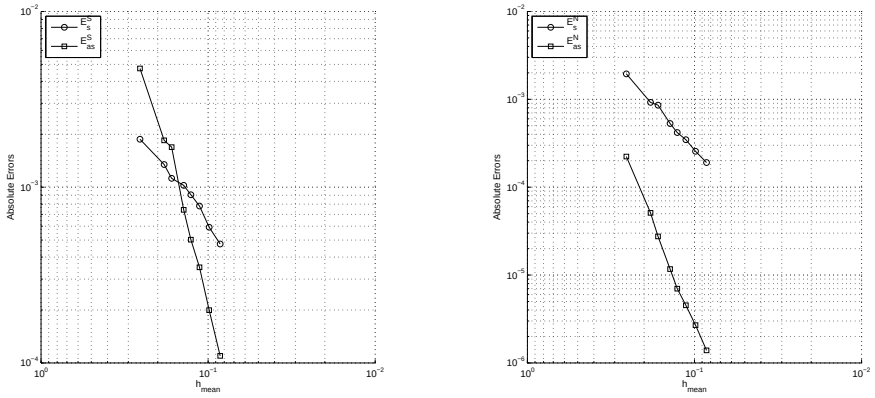

FIG. 4. *Absolute numerical errors for the solutions of the boundary integral equations linked to the operators $\mathcal{S}_s$ and $\mathcal{S}_{as}$ (left) and to the operators $\mathcal{N}_s$ and $\mathcal{N}_{as}$ (right).*

four boundary integral equations, each associated with one of the new boundary integral operators on the disk, their known exact solutions, as given by Proposition 3.12, the numerical approximations, and the numerical errors.

In what follows, the error convergence is shown for decreasing mean edge size of the mesh. Figure 4 shows the convergence of the numerical error defined in Table 1 for the four boundary integral equations. The decreasing numerical error, as shown in Figure 4, confirms the capacity of the proposed numerical schema and its implementation of solving the new boundary integral equations arising from the new operators from Definition 3.11.

4.3. Preconditioning the single layer and the hypersingular boundary integral operators on the disk. Once the numerical implementation has been shown to be effective, we take interest in the preconditioning properties of the matrices associated with the bilinear forms involved in the finite-dimensional variational formulations. We define basis projection matrices taking the bilinear form d from Theorem 2.1 to be the duality product $\langle \cdot\,, \cdot \rangle_{\mathbb{D}}$.

DEFINITION 4.9 (basis projection Galerkin matrices). *Let us define the following basis projection Galerkin matrices:*

$$\boldsymbol{D}_{1,h}[i,j] = \langle \chi_i, \kappa_j \rangle_{\mathbb{D}_h} \quad \textit{and} \quad \boldsymbol{D}_{2,h}[i,j] = \langle \chi_i^0, \kappa_j^0 \rangle_{\mathbb{D}_h}.$$

We now follow Theorem 2.1 in building preconditioned Galerkin matrices associated with the four new boundary integral operators, using them pairwise as mutual preconditioners:

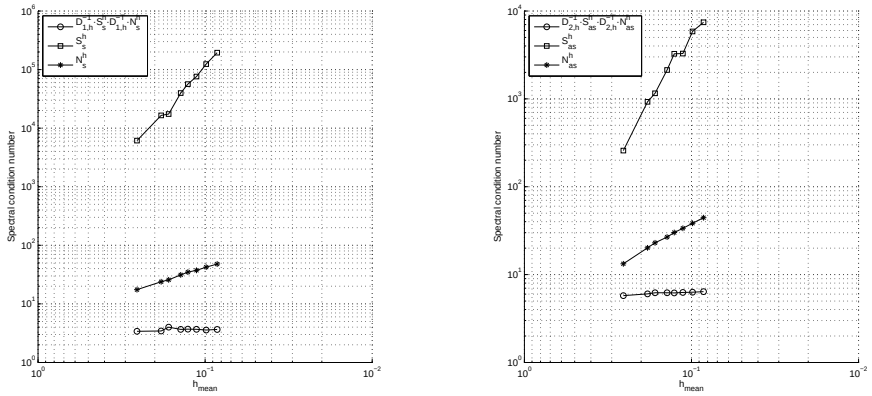

FIG. 5. *Spectral condition number of the $\boldsymbol{S}_s^h$ matrix , the $\boldsymbol{N}_s^h$ matrix, and their performance as mutual preconditioners (left). Spectral condition number of the $\boldsymbol{S}_{as}^h$ matrix, the $\boldsymbol{N}_{as}^h$ matrix, and their performance as mutual preconditioners (right).*

$$\boldsymbol{D}_{1,h}^{-1}\boldsymbol{S}_s^h\boldsymbol{D}_{1,h}^{-T}\boldsymbol{N}_s^h \quad \text{and} \quad \boldsymbol{D}_{2,h}^{-1}\boldsymbol{S}_{as}^h\boldsymbol{D}_{2,h}^{-T}\boldsymbol{N}_{as}^h. \tag{16}$$

We examine the evolution of the spectral condition number of these matrices for decreasing mean edge size of the mesh. Figure 5 shows the spectral condition number of the previously defined matrices exhibiting their performance as mutual preconditioners. It is remarkable that the new boundary integral operators perform experimentally as asymptotically bounded mutual operator preconditioners, achieving low spectral condition numbers.

It is remarkable that the pair of matrices associated with the so-called symmetric operators and the pair of matrices associated with the so-called antisymmetric operators act experimentally as optimal mutual preconditioners, providing bounded condition numbers independently of the refinement of the mesh. This suggests that the bilinear forms induced by the operators are continuous and coercive in spaces linked by duality, as requested by Theorem 2.1 for optimality in preconditioning. It is also remarkable that the asymptotically bounded conditioned number achieved is low, as suggested by the Calderón-type identities provided. Finally, it is also remarkable that the duality pairing of the basis functions from U_h and V_h, and the basis functions from U_h^0 and V_h^0, appears to be stable in the sense defined by (3).

Having noted the mutual preconditioning capabilities of the new boundary integral operators on the disk, we interest ourselves in the possibility of using these matrices as preconditioners for the Galerkin matrices arising from the variational formulation of the boundary integral equations for operators $\mathcal{S}$ and $\mathcal{N}$, linked with the symmetric Dirichlet and antisymmetric Neumann problems on the disk.

DEFINITION 4.10 (Galerkin matrices of the weakly singular and hypersingular operators). *We define the matrices associated with the bilinear form for the weakly singular and hypersingular boundary integral operator:*

$$\boldsymbol{S}^h[i,j] = \langle \mathcal{S}\,\kappa_i, \kappa_j\rangle_{\mathbb{D}_h} \text{ and } \boldsymbol{N}^h[i,j] = \langle \mathcal{N}\,\chi_i^0, \chi_j^0\rangle_{\mathbb{D}_h} + \beta\langle\chi_i^0, 1\rangle_{\mathbb{D}_h}\langle\chi_j^0, 1\rangle_{\mathbb{D}_h}. \tag{17}$$

As before, a parameter $\beta \in \mathbb{R}^+$ is used to restrict the space involved in order to account for the kernel space of the hypersingular boundary integral operator.

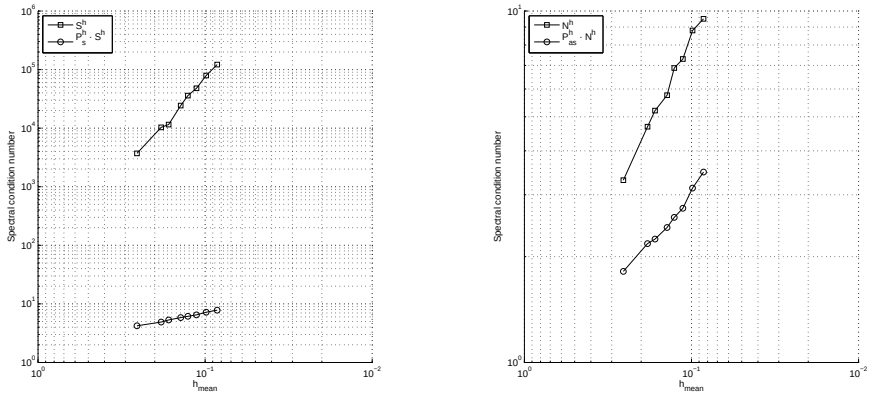

FIG. 6. *Spectral condition number of the $\boldsymbol{S}^h$ matrix and the performance of the $\boldsymbol{P}_s^h$ matrix as preconditioner (left). Spectral condition number of the $\boldsymbol{N}^h$ matrix and the performance of the $\boldsymbol{P}_{as}^h$ matrix as preconditioner (right).*

DEFINITION 4.11 (preconditionning matrices). *We define preconditioning matrices for the weakly singular and hypersingular operator matrices based on $\mathcal{N}_s$ and $\mathcal{S}_{as}$, respectively. Taking the expressions from Theorem* 2.1,

$$\boldsymbol{P}_s^h = \boldsymbol{D}_{1,h}^{-1}\boldsymbol{N}_s^h\boldsymbol{D}_{1,h}^{-T} \text{ and } \boldsymbol{P}_{as}^h = \boldsymbol{D}_{2,h}^{-1}\boldsymbol{S}_{as}^h\boldsymbol{D}_{2,h}^{-T}. \tag{18}$$

We use $\boldsymbol{P}_s^h$ to precondition $\boldsymbol{S}^h$ and $\boldsymbol{P}_{as}^h$ to precondition $\boldsymbol{N}^h$. Figure 6 shows the spectral condition numbers of the Galerkin matrices associated with the weakly singular and hypersingular boundary integral operators and the performance of the defined preconditioners for a mesh refinement measured by diminishing mean edge sizes.

In this case, the condition number is greatly decreased, specially for the $\boldsymbol{S}^h$ matrix, although the preconditioning method is not asymptotically bounded, i.e., is not optimal. This is the consequence of $\mathcal{S}_{as}$ and $\mathcal{N}_s$ not being exact inverses for $\mathcal{N}$ and $\mathcal{S}$, nor being inducers of coercive bilinear forms in the dual spaces of $\widetilde{H}^{1/2}(\mathbb{D})$ and $\widetilde{H}^{-1/2}(\mathbb{D})$: $H^{-1/2}(\mathbb{D})$ and $H^{1/2}(\mathbb{D})$. The performance of the preconditioner linked to $\mathcal{N}_s$ which is only moderate. This is due to the condition number of matrix $\boldsymbol{N}^h$ already being improved because of the augmentation parameter β described in Definition 4.10.

4.4. Extension to other shapes. The preconditioning effect of matrices $\boldsymbol{P}_s^h$ and $\boldsymbol{P}_{as}^h$ is achieved by selecting kernels K_s^{hs} and K_{as}^{ws} that induce integral operators that, while not providing exact inverses for $\mathcal{S}$ and $\mathcal{N}$, have some desirable features. Mainly, they behave similarly to what the inverses' behavior was in the two-dimensional case and in relation to the known behavior of the jump of traces, as stated in Remark 3.1, related to $w(\rho)$ and $1/w(\rho)$. Also, the weight function w was intimately related to the relation between the sphere and the disk. This role manifested in the fact that vertical projection of point $\mathbf{x}$ on the disk onto the sphere, $\mathbf{x}^{\pm}$, were separated by the quantity $w(\mathbf{x})$. In this section we use these elements to extend the action of the defined preconditioners by preserving the role they had for disk $\mathbb{D}$.

Let us define the function

$$w_\Gamma(\mathbf{x}) = \sqrt{\operatorname{dist}(\mathbf{x}, \partial\Gamma)} \quad \text{for } \mathbf{x} \in \Gamma. \tag{19}$$

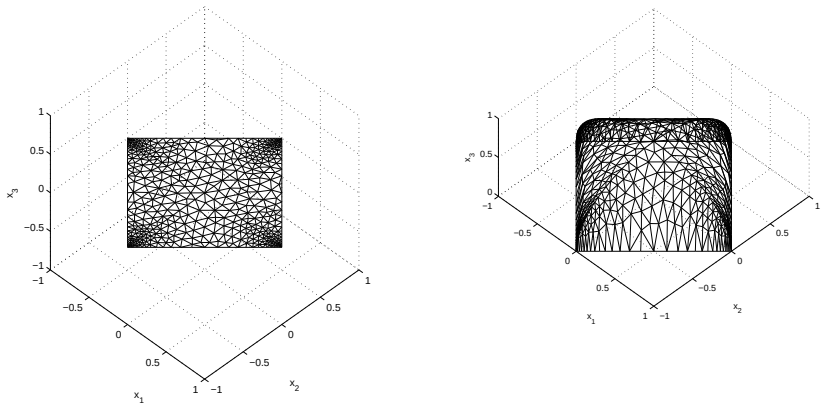

FIG. 7. *Discretized domain Γ_h for a squared-shaped screen (left) with its chosen projection Γ_h^+ (right) for the mesh set.*

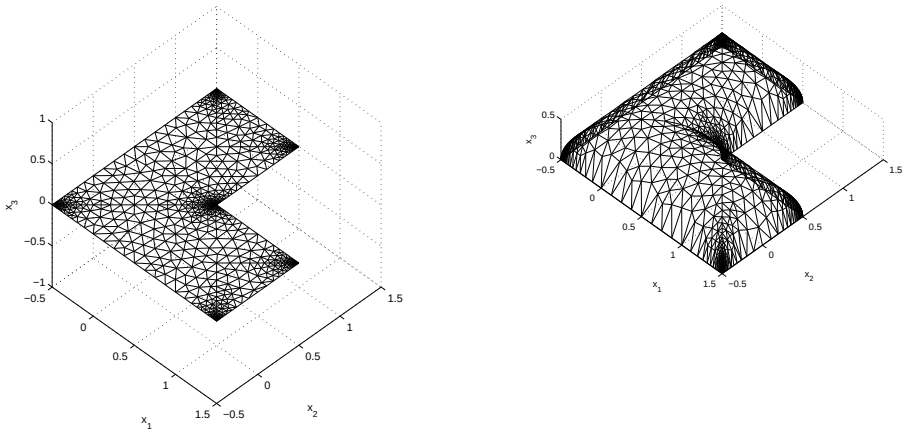

FIG. 8. *Discretized domain Γ_h for an L-shaped screen (left) with its chosen projection Γ_h^+ (right).*

We replace in the previous procedure w with w_Γ. This implies that the upper and lower meshes, now Γ_h^+ and Γ_h^-, and the vertical projection of the triangles of Γ_h are now to be governed by the point projection $\mathbf{x}^\pm = (x_1, x_2, \pm w_\Gamma(\mathbf{x}))$. This results in new upper and lower meshes and triangle projections $K^\pm$ when used in the boundary element computations. We also replace w with w_Γ whenever present in the numerical scheme, i.e., in (15).

To put this idea to the test, we consider two different screens: a square-shaped and an L-shaped screen. Figures 7 and 8 show the discretized domain for the square-shaped and the L-sphape screens, Γ_h, along with their corresponding projected upper mesh Γ_h^+. Figures 9 and 10 show the evolution of the spectral condition number for the case of the square-shaped and L-shaped screens, respectively, using the proposed method, i.e., replacing w with w_Γ and thus also upper and lower meshes (and thus triangle projections) and using preconditioner matrices from Definition 4.11.

The condition number has greatly improved, although it presents anomalies in its evolution as the mean edge size of the mesh diminishes. This is due to the fact that the broken angles on the edge of the screen introduce other singularities on the jump

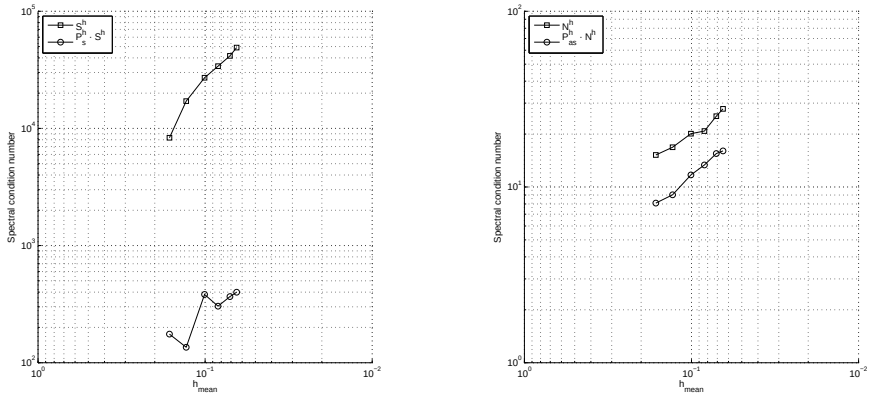

FIG. 9. *Spectral condition number of the* $\boldsymbol{S}^h$ *matrix and the performance of the* $\boldsymbol{P}_s^h$ *matrix as a preconditioner for the square-shaped screen (left). Spectral condition number of the* $\boldsymbol{N}^h$ *matrix and the performance of the* $\boldsymbol{P}_{as}^h$ *matrix as a preconditioner for the square-shaped screen case (right).*

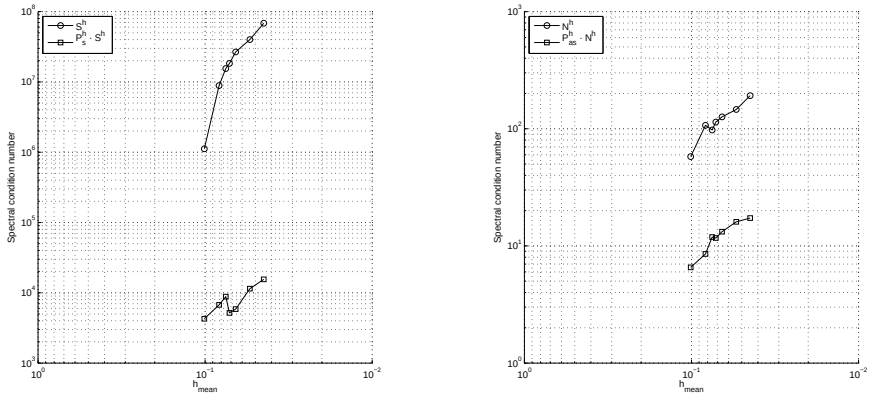

FIG. 10. *Spectral condition number of the* $\boldsymbol{S}^h$ *matrix and the performance of the* $\boldsymbol{P}_s^h$ *matrix as a preconditioner for the L-shaped screen (left). Spectral condition number of the* $\boldsymbol{N}^h$ *matrix and the performance of the* $\boldsymbol{P}_{as}^h$ *matrix as a preconditioner for the L-shaped screen (right).*

of the traces, not described so far and falling outside the scope of this article. These anomalies are sensitive to the values α and β chosen to eliminate kernel spaces. The preconditioning effect for matrix $\boldsymbol{N}^h$ was again moderate, especially for the case of the square-shaped screen.

5. Conclusions. We have proposed new integral kernels, taking as hints the forms of the kernels of the exact inverses for $\mathcal{S}$ and $\mathcal{N}$ when the screen was the segment in $\mathbb{R}^2$ and the known behavior of the jump of the Dirichlet and Neumann traces for the Laplace problem in three dimensions. These new integral kernels preserve the radial behavior (on the ρ direction), in comparison with the bidimensional case, using a weight function w in the case of the disk screen. These kernels give rise to integral operators for which the mapping properties and Calderón-type identities were found. The particular choice of the coefficients of the series of the integral kernels also allowed for explicit and closed-form variational expressions that were suitable for use in boundary element methods. Numerical schemes were proposed for the boundary element computation of the associated bilinear forms. These schemes were tested ensuring

their correct use approximations and their implementation. The Galerkin matrices arising from the proposed boundary integral operators were shown to be optimal mutual preconditioners, suggesting that the selected basis for the finite-dimensional variational formulations had stable pairings and that the new boundary integral operators induce coercive bilinear forms in some yet undefined Hilbert spaces. These Galerkin matrices associated with the new operators were then used to precondition the ones arising from the bilinear forms induced by $\mathcal{S}$ and $\mathcal{N}$, which are needed for the resolution of the Dirichlet and Neumann problem. This method showed a significant decrease of the condition number, although suboptimal, suggesting that the new integral operators do not furnish coercive bilinear forms in the Sobolev spaces of the given Dirichlet and Neumann data. The preconditioning effect was better observed for the Galerkin matrix associated with $\mathcal{S}$, as the one associated with $\mathcal{N}$ had much better condition numbers. The technique was extended to other shapes, changing the weight function w to reflect the behavior of the jump of the traces locally near the edges of the screens. This method proved to greatly reduce the condition number in some cases, opening the way to precondition other complex-shaped screens. The effect of the proposed management of the condition number on the number of iterations used to solve boundary integral equations with boundary element methods will depend on the iterative method chosen, although it is ensured to improve with decreased condition numbers.

REFERENCES

[1] A. Bendali and C. Devys, *Calcul numérique du rayonnement de cornets électromagnétiques dont l'ouverture est partiellement remplie par un diélectrique*, Onde électrique, 66 (1986), pp. 77–81.

[2] G. H. Golub and C. F. V. Loan, *Matrix Computations*, 4th ed., Johns Hopkins Stud. Math. Sci., Johns Hopkins University Press, 2013.

[3] R. Hein, *Green's Functions and Integral Equations for the Laplace and Helmholtz Operators in Impedance Half-Spaces*, Ph.D. thesis, École Polytechnique, 2010.

[4] R. Hiptmair, *Operator preconditioning*, Comput. Math. Appl., 52 (2006), pp. 699–706.

[5] R. Hiptmair, C. Jerez-Hanckes, and C. Urzúa-Torres, *Mesh-independent operator preconditioning for boundary elements on open curves*, SIAM J. Numer. Anal., 52 (2014), pp. 2295–2314.

[6] R. Hiptmair, C. Jerez-Hanckes, and C. Urzúa-Torres, *Optimal Operator Preconditioning for Hypersingular Operator over 3d Screens*, Tech. report 2016-09, Seminar for Applied Mathematics, ETH Zürich, 2016.

[7] G. C. Hsiao and W. L. Wendland, *Boundary Integral Equations*, Springer, New York, 2008.

[8] C. Jerez-Hanckes and J.-C. Nédélec, *Explicit variational forms for the inverses of integral logarithmic operators over an interval*, SIAM J. Math. Anal., 44 (2012), pp. 2666–2694.

[9] X.-F. Li and E.-Q. Rong, *Solution of a class of two-dimensional integral equations*, J. Comput. Appl. Math., 145 (2002), pp. 335–343.

[10] S. K. Lintner and O. P. Bruno, *A generalized Calderón formula for open-arc diffraction problems: Theoretical considerations*, Proc. Roy. Soc. Edinburgh Sect. A., 145 (2015), pp. 331–364.

[11] W. McLean and O. Steinbach, *Boundary element preconditioners for a hypersingular integral equation on an interval*, Adv. Comput. Math., 11 (1999), pp. 271–286.

[12] W. C. H. McLean, *Strongly Elliptic Systems and Boundary Integral Equations*, Cambridge University Press, Cambridge, UK, 2000.

[13] Y. Mi and M. Aliabadi, *Three-dimensional crack growth simulation using BEM*, Computers & Structures, 52 (1994), pp. 871–878.

[14] J.-C. Nédélec, *Acoustic and Electromagnetic Equations: Integral Representations for Harmonic Problems*, Appl. Math. Sci., Springer, New York, 2001.

[15] A. Portela, M. Aliabadi, and D. P. Rooke, *Dual boundary element incremental analysis of crack propagation*, Computers & Structures, 46 (1993), pp. 237–247.

[16] S. A. Sauter and C. Schwab, *Boundary element methods*, in Boundary Element Methods, Springer, New York, 2010, pp. 183–287.

[17] Y. Shestopalov, Y. Smirnov, and E. Chernokozhin, *Logarithmic Integral Equations in Electromagnetics*, VSP, Utrecht, 2010.
[18] O. Steinbach, *Stability Estimates for Hybrid Coupled Domain Decomposition Methods*, Lecture Notes in Math., 1809, Springer, New York, 2003.
[19] E. P. Stephan, *Boundary integral equations for screen problems in IR*3, Integral Equations Operator Theory, 10 (1987), pp. 236–257.